

REPUBLIC OF TURKEY
YILDIZ TECHNICAL UNIVERSITY
GRADUATE SCHOOL OF SCIENCE AND ENGINEERING

DESIGN AND APPLICATION OF A LOW SOOT EMISSION
TARGETED COMBUSTION CHAMBER FOR DIESEL ENGINES

Caner KARACA

MASTER OF SCIENCE THESIS
Department of Mechanical Engineering
Automotive Program

Advisor
Assoc. Prof. Dr. Levent YÜKSEK

August, 2021

REPUBLIC OF TURKEY
YILDIZ TECHNICAL UNIVERSITY
GRADUATE SCHOOL OF SCIENCE AND ENGINEERING

DESIGN AND APPLICATION OF A LOW SOOT EMISSION
TARGETED COMBUSTION CHAMBER FOR DIESEL ENGINES

Caner KARACA

MASTER OF SCIENCE THESIS
Department of Mechanical Engineering
Automotive Program

Advisor
Assoc. Prof. Dr. Levent YÜKSEK

August, 2021

REPUCLIC OF TURKEY

YILDIZ TECHNICAL UNIVERSITY

GRADUATE SCHOOL OF SCIENCE AND ENGINEERING

**DESIGN AND APPLICATION OF A LOW SOOT EMISSION
TARGETED COMBUSTION CHAMBER IN DIESEL ENGINES**

A thesis submitted by Caner KARACA in partial fulfillment of the requirements for the degree of MASTER OF SCIENCE is approved by the committee on 23/08/2021 in Department of Mechanical Engineering, Automotive Program

Assoc. Prof. Dr. Levent YÜKSEK

Yıldız Technical University

Advisor

Approved by the Examining Committee

Assoc. Prof. Dr. Levent YÜKSEK, Advisor

Yıldız Technical University

Assoc. Prof. Dr. Orkun ÖZENER, Member

Yıldız Technical University

Asst. Prof. Dr. Barış DOĞRU, Member

İstanbul Technical University

I hereby declare that I have obtained the required legal permissions during data collection and exploitation procedures, that I have made the in-text citations and cited the references properly, that I have not falsified and/or fabricated research data and results of the study and that I have abided by the principles of the scientific research and ethics during my Thesis Study under the title Design and Application of a Low Soot Emission Targeted Combustion Chamber in Diesel Engines supervised by my supervisor, Assoc. Prof. Levent YÜKSEK. In the case of a discovery of false statement, I am to acknowledge any legal consequence.

Caner KARACA

Signature

Dedicated to my mother

ACKNOWLEDGEMENTS

I would like to thank my supervisor Assoc. Prof. Levent YÜKSEK for his support and guidance throughout this study.

I want to thank Gökhan TANRISEVER for his support during the experimental parts of this study. Special thanks to Hüseyin SİPAHİ and Serkan KARAKAYA of Mita-Kalıp Inc. and, Aziz ŞENER and Ufuk ŞENER of Aksa Makina Inc. for their contributions in my experimental works.

I want to thank all of my colleagues from TÛMOSAN Teknoloji and Mühendislik Inc. for their support, patience and understanding.

Last but not least, I want to thank my family for standing up for me during our tough times.

TABLE OF CONTENTS

LIST OF SYMBOLS	vii
LIST OF ABBREVIATIONS	ix
LIST OF FIGURES	x
LIST OF TABLES	x
ABSTRACT	xiii
ÖZET	xv
1 INTRODUCTION	1
1.1 Literature Review.....	1
1.2 Objective of the Thesis	5
1.3 Hypothesis	6
2 COMBUSTION CHAMBER DESIGN IN CI ENGINES	7
2.1 Working Principle of CI Engines.....	7
2.1.1 Intake Stroke.....	7
2.1.2 Compression Stroke	8
2.1.3 Expansion Stroke	8
2.1.4 Exhaust Stroke	9
2.2 Combustion in CI Engines	9
2.2.1 Fuel Spray Behaviour	10
2.2.2 Combustion Phases in Diesel Engines.....	11
2.3 Pollutant Formation in Diesel Engines	13
2.3.1 NO _x Emissions	14
2.3.2 Carbon Monoxide (CO) Emissions	15
2.3.3 Hydrocarbon (HC) Emissions	15
2.3.4 Soot Emissions	15
2.3.5 Soot-NO _x Trade-off.....	16
2.4 Combustion System Design in Diesel Engines	16
2.4.1 Engine Parameters	17

2.4.2	Piston Bowl Design Parameters	21
2.4.3	Air Flow Parameters.....	24
2.4.4	Fuel Injection Parameters.....	26
2.5	Types of Combustion Chambers	32
2.5.1	Direct Injection Combustion Chambers	32
2.5.2	Indirect Injection Combustion Chambers	33
3	COMPUTATIONAL FLUID DYNAMICS SIMULATIONS	35
3.1	Mathematical Background	35
3.1.1	Conservation of Mass	36
3.1.2	Conservation of Momentum.....	36
3.1.3	Conservation of Energy:.....	37
3.1.4	Turbulence Model.....	37
3.2	Engine Model Setup.....	38
3.2.1	Stepped Lip Combustion Chamber	39
3.3	CFD Simulations	40
3.4	CFD Results.....	43
4	EXPERIMENTAL WORK	46
4.1	Methodology Used for Piston Production	46
4.2	DC Motor Specifications.....	49
4.3	Specifications of Emission Measurement Devices	50
4.4	Engine Operation Conditions	52
4.5	Emission Results	53
5	RESULTS AND DISCUSSION	57
	REFERENCES	59
	PUBLICATIONS FROM THE THESIS	62

LIST OF SYMBOLS

ω_s	Angular Velocity of the Intake Air
D_b	Bowl diameter (mm)
$V_{\text{clearance}}$	Clearance Volume (mm^3)
r_c	Compression Ratio
A_c	Cross Sectional Area of the Cylinder (mm^2)
B	Cylinder Bore (mm)
V_{dead}	Dead Volume at Top Dead Center (mm^3)
ρ	Density (g/mm^3)
φ	Dissipation Functoin
ε	Dissipation Rate
Z	Distance Between the Piston Top and the Cylinder Head (mm)
μ	Dynamic Viscosity (Pa.s)
S_M	Momentum Source
n	Number of Cylinders
V_{bowl}	Piston Bowl Volume (mm^3)
S_p	Piston Speed (m/s)
N	Rotational Speed of Crankshaft (rpm)
v_{sq}	Squish Velocity (m/s)
L	Stroke (mm)
R_S	Swirl Ratio
T	Temperature (K)

t	Time (s)
V_{engine}	Total Cylinder Displacement (mm^3)
i	Total Energy (Joule)
τ	Total Stress
k	Turbulent Kinetic Energy
u	Velocity Vector

LIST OF ABBREVIATIONS

BSFC	Brake Specific Fuel Consumption
BTDC	Before Top Dead Center
CA	Crank Angle
CFD	Computational Fluid Dynamics
CI	Compression Ignition
CLD	Chemiluminescence Detector
EVO	Exhaust Valve Opening
FID	Flame Ionization Detector
FSN	Filter Smoke Number
IMEP	Indicated Mean Effective Pressure
IVC	Intake Valve Closure
NDIR	Nondispersive Infrared Analyzer
PIV	Particle Image Velocimetry
RoHR	Rate of Heat Release
ULPC	Ultra Low Particulate Combustion

LIST OF FIGURES

Figure 2.1 Illustration of the intake stroke in CI engines [9].....	7
Figure 2.2 Illustration of the compression stroke in CI engines [9].....	8
Figure 2.3 Illustration of the expansion stroke in CI engines [9]	8
Figure 2.4 Illustration of the exhaust stroke in CI engines [9]	9
Figure 2.5 Illustration of an injection into a combustion chamber [9]	10
Figure 2.6 Total heat release rates in a diesel combustion [9]	13
Figure 2.7 Temperature distribution and emission formation on a fuel spray [12].....	14
Figure 2.8 Demonstration of soot-NOx trade-off [13].....	16
Figure 2.9 Geometric view of an cylinder piston mechanism [9]	18
Figure 2.10 Illustration of k-factor for both high and low compression ratios [14].....	19
Figure 2.11 Demonstration of piston combustion chamber design parameters ..	23
Figure 2.12 Illustration of the lip radius on a bowl [14]	24
Figure 2.13 Various types of inlet port designs [9]	25
Figure 2.14 Squish flow on a direct injection combustion chamber [9]	25
Figure 2.15 Demonstation of the measures in order to calculate squish velocities [9].....	26
Figure 2.16 Tumble flow in a combustion chamber [10]	26
Figure 2.17 Fuel spray structure [9]	27
Figure 2.18 Illustration of a spray targeting method [14].....	30
Figure 2.19 Various options for fuel targeting and nozzle configurations[15] ...	30
Figure 2.20 Volvo wave piston model [16]	31
Figure 2.21 Lateral swirl combustion chamber [17]	31
Figure 2.22 Lateral swirl formation mechanisms [17]	32
Figure 2.23 Various types of direct injection combustion chambers [9]	32
Figure 2.24 Various indirect injection combustion chamber designs.....	33
Figure 3.1 Mexican hat combustion chamber of Antor 6LD400	39

Figure 3.2	Illustration of the stepped lip combustion chamber	39
Figure 3.3	Stepped lip bowl design for Antor 6LD400	40
Figure 3.4	Valve lift profiles of Antor 6LD400	41
Figure 3.5	Illustration of GT Power interface	42
Figure 3.6	Illustration of the 1D model for the test engine	42
Figure 3.7	Validation of in-cylinder pressure between 1D and CFD analyses	43
Figure 3.8	Mexican hat bowl at -50° CA.....	43
Figure 3.9	Stepped lip bowl at -50° CA	43
Figure 3.10	Mexican hat bowl at -25° CA.....	44
Figure 3.11	Stepped lip bowl at -25° CA	44
Figure 3.12	Mexican hat bowl at top dead center	44
Figure 3.13	Stepped lip bowl at top dead center.....	44
Figure 4.1	Machining dimensions and tolerances for stepped lip design.....	46
Figure 4.2	Machining process of stepped lip bowl.....	47
Figure 4.3	Machined stepped lip combustion chamber	48
Figure 4.4	Technical drawing of the parametric bowl volume for 0.55 mm machining	48
Figure 4.5	Top surface machining process of the second piston	49
Figure 4.6	Selected DC motor for experimental work	50
Figure 4.7	CO Emission results	53
Figure 4.8	CO ₂ Emission results	54
Figure 4.9	O ₂ Emission results	54
Figure 4.10	HC Emission results	55
Figure 4.11	NO _x Emission results.....	55
Figure 4.12	Soot emission results	56
Figure 4.13	Calculated fuel consumption results	56

LIST OF TABLES

Table 3.1	Specifications of the engine selected for this study.....	38
Table 3.2	Valve timings of Antor 6LD400	41
Table 3.3	Boundary conditions for CFD Analyses obtained from 1D analysis.....	42
Table 4.1	Specification of DC Motor	50
Table 4.2	Specifications of AVL Digas 4000	51
Table 4.3	Specifications of AVL 415S.....	52
Table 4.4	Steady state experiment conditions.....	53

Design and Application of a Low Soot Emission Targeted Combustion Chamber for Diesel Engines

Caner KARACA

Department of Mechanical Engineering

Master of Science Thesis

Supervisor: Assoc. Prof. Dr. Levent YÜKSEK

Diesel engine emission levels are strictly regulated over the year. Meeting these emission regulations has always been a challenging job for diesel engine developers. Considering the cost problems and complexities of diesel engine aftertreatment systems, in order to meet the soot and NO_x levels, engineers had to come up with alternative design solutions. Since changing the combustion chamber design has always been a more cost effective and easily applicable solution compared to complex diesel engine aftertreatment devices, various chamber designs have been researched and tested by engineers. The geometrical shape of the combustion chamber is particularly significant in order to improve the turbulent flow structures and in-cylinder flow velocities that would affect combustion efficiency and engine-out emissions. Two of the most widely used designs are mexican hat and stepped-lip chambers. The stepped lip design in particular, has been widely investigated due to their function of promoting recirculating flow structures which enhances fuel-air mixing and resulting with lower soot emission levels. The main objective of this thesis is to investigate the effect of stepped-lip combustion chamber design and compare the in-cylinder vortex structures with a conventional mexican hat chamber. A 3D CFD model has been carried out in order to understand the in-cylinder flow structures and vortex

formations. Then an experimental study has been conducted with a single cylinder diesel engine with an in-line pump injection system and soot emission levels of both mexican hat and stepped lip combustion chambers have been compared.

Keywords: Diesel engine, combustion chamber, stepped lip, CFD analysis, soot emission

YILDIZ TECHNICAL UNIVERSITY

GRADUATE SCHOOL OF SCIENCE AND ENGINEERING

Dizel Motorlarda Düşük İş Emisyonu Hedefli Yanma Odasının Tasarımı ve Uygulaması

Caner KARACA

Makine Mühendisliği Anabilim Dalı

Yüksek Lisans Tezi

Danışman: Doç. Dr. Levent YÜKSEK

Dizel motorların emisyon seviyeleri yıllardır sıkı bir şekilde kontrol edilmektedir. Bu emisyon seviyelerini karşılamak, dizel motor geliştiricileri için her zaman zor bir iş olmuştur. Dizel motorlarda kullanılan emisyon azaltıcı sistemlerinin maliyeti ve kontrol problemleri ele alındığında, mühendisler, is ve azotoksit emisyonlarını düşürmek için alternatif tasarım çözümleri bulmak zorunda kalmıştır. Bir dizel motorda yanma odasının tasarımını değiştirmek, emisyon azaltıcı sistemlerin maliyet ve kontrol problemleri ele alındığında daha ucuz ve kolaylıkla uygulanabilir bir yöntemdir. Dolayısıyla dizel motor tarihinde pek çok yanma odası tasarımı incelenmiş ve test edilmiştir. Piston yanma odasının geometrik şekli, silindir içi türbülans yapılarını ve akış hızlarını doğrudan etkilediği için, dizel motorlarda performans ve emisyon seviyelerinin kontrolü açısından doğrudan etkiye sahiptir. Günümüzde en çok kullanılan yanma odası tasarımları meksika şapkası geometrisi ve kademeli yanma odası geometrisidir. Özellikle kademeli yanma odası geometrisinin silindir içi hava hareketlerine, silindir içi hava-yakıt karışımına etkisi ve is emisyon seviyelerine etkisi detaylı olarak araştırılmıştır. Bu tez kapsamında, kademeli yanma odası geometrisine sahip bir yanma odasının silindir içi vorteks oluşumuna etkisi incelenmiş ve geleneksel meksika şapkasıyanma odası ile karşılaştırılmıştır. 3 boyutlu hesaplamalı akış dinamiği araçları kullanılarak, soğuk akış modelleri iki yanma odası tasarımı için kurulmuş

ve vorteks oluřumları karřılařtırılmıřtır. Soėuk akıř analizleri alıřmalarından elde edilen sonular doėruľtunda, kademeli yanma odasına sahip bir piston modeli üretilip tek silindirli ve mekanik enjeksiyon sistemine sahip bir motorda test edilmiřtir. Testler sonucunda kademeli yanma odası geometrisinin is emisyonlarına etkisi gözlemlenip, sonular, meksika řapkası yanma odası geometrisi ile alınan emisyon seviyeleri ile karřılařtırılmıřtır.

Anahtar kelimeler: Dizel motor, yanma odası, kademeli yanma odası, CFD analiz, is emisyonu

1.1 Literature Review

Leach and Ismail have investigated the emission and performance of stepped lip combustion chamber design on a single cylinder 0,5 L light duty diesel engine with 15.4:1 compression ratio. A conventional re-entrant bowl and a stepped lip bowl have simulated and tested at two steady speed load operating conditions, one at a low load(1500 rpm/6.8 bar IMEP), one at a medium load(1750 rpm/13.5 bar IMEP). Additionally, full load curves were run at four different engine speeds with 1500 rpm, 2000 rpm, 3000 rpm, 4000 rpm. A CFD model is defined between IVC and EVO as an insight into details of the spray mechanisms, mixing, and combustion processes at each operating point and to explain experimental combustion and emission trends. Results suggested that there is no significant difference in NO_x and soot emission at part load and a minor penalty in NO_x emissions at some full loads. It is also pointed in the paper that comparisons between experiments and CFD predictions are challenging due to post-flame oxidations associated with the high temperature exhaust gas[1].

Ford Motor Co. has investigated 2 different combustion chamber designs for their 6.7 liters V-8 Powerstroke diesel engine. One being a conventional re-entrant bowl and the other a chamfered bowl. 3-D CFD analyses with spray and combustion models have been run in AVL FIRE at 4 operating conditions to optimize the fuel efficiency, NO_x and soot performances. A merit function has defined based on IMEP, soot and NO_x values calculated from CFD runs. IMEP has given the highest weighting value as it would be the divisor in fuel economy and emission calculations. Due to the fact that IMEP value has a critical factor in the merit function, the chamber that could minimize heat losses is likely to have higher merit numbers. It was observed from the CFD runs that the chamfered bowl tends to lose less heat to the cylinder liner and thus resulting in higher merit value. Then, various combinations of combustion chambers, swirl numbers and injector

parameters have been modelled and tested. It was understood from the paper that the low swirl combustion system with the chamfered chamber design has performed better soot and BSFC levels[2].

Benajes, Pastor and Garcia have investigated the effect of piston bowl geometry on reactivity controlled compression ignition and emissions in a heavy duty diesel engine. A single cylinder 1.806 L engine which has 14.4:1 compression ratio with dual fuel injection system has used in testing. 3 piston geometries has been tested, one being a conventional re-entrant bowl, one being a stepped bowl due to its ability to modify the squish flow in order to enhance oxidation in this region, and the other one being a bathtub model aiming a greater reduction in piston surface area for lowering heat transfer losses. 3 load classes at constant engine speed have been described as low, medium and high in testing. Two different injection strategies with dual fuel combinations have been described for each load conditions. Results suggested that; at low load, standard re-entrant bowl enhanced the mixing process providing earlier SOC than bathtub and stepped models. At medium load, the reduced heat transfer losses due to the lower are to volume ratio of bathtub piston promoted higher combustion temperature peaks, which resulted with reduced combustion losses and fuel economy while maintaining the soot and NO_x levels under EURO VI levels. At high load, stepped piston geometry showed better results in terms of NO_x, soot and fuel consumption levels[3].

Perini and Zha have studied the effects of piston geometry has on a swirl supported light duty diesel engine. 3 chamber designs have been prepared. 2 of them being re-entrant with one having valve cut-outs. The third design selected to be a stepped design. A computational model has been introduced in FRESKO in order to analyze the in-cylinder swirl vortex, bulk flow and turbulence availability close to top dead center. Then the models have been experimented with a 477.2 mm³ single cylinder diesel engine which is equipped with an in-cylinder particle image velocimetry(PIV). Throttle plates are fitted to the intake ports to arbitrarily adjusted the swirl ratio, allowing it to sweep from $R_s = 1.5$ to $R_s = 5.5$. Flow analyses have implied that the conventional re-entrant bowl had

stronger squish flow due to its enclosed shape which leads to 10% stronger swirl at near-TDC. It can also be understood from the analyses that stepped bowl allows larger swirl axis tilt and lesser flow axisymmetry which results in higher turbulence levels but faster turbulence dissipation during intake and compression strokes [4].

Eder, Kemmer, Lückert and Sass from Mercedes company has launched the OM 654 engine family with the usage of a stepped lip piston geometry. The reason behind the usage of stepped geometry has explained to be minimizing the dead space that can not be reached by the injection jets in order to achieve maximum air utilization which results in low soot emission levels. Due to the modified flow conditions, the heat loss through cylinder walls has reduced and temperature distribution at cylinder head has homogenized which resulted in relieve in the highly stressed valve lands[5].

Lee and Kim have studied the optimization bowl shape design for engine-out PM reduction in a heavy-duty diesel engine. The base combustion chamber is selected as a ULPC design due to achieving high air utilization via separating fuel jets via the lower lip of the combustion chamber. Effects of bowl diameter, bowl lip height and pip height on soot emissions and BSFC are investigated with a CFD code using KIVA3v-rel2 coupled with Chemkin 2.0. By studying the analyses; the most dominant design factor has seen to be the bowl width due to better oxygen utilization. Lip height also had an important role in order to determine the optimal portion of fuel split. Approximately 40 to 60 fuel split ratio found out to be the optimal situation which means 40% of the fuel is directed to the upper region of the bowl while 60% remain under the lip region. The optimum model is experimented in a 6 L diesel engine with 17.4:1 compression ratio. A steady state test cycle defined as C1-8 mode in ISO 8178 has been conducted. Results showed 60% reduction in PM emission[6].

Dolak, Shi and Reitz have computationally investigated the stepped bowl design for a light duty engine which is operating at low load condition. The research is focused on exploring combinations of spray targeting by using split injections with

stepped bowl configuration along with interactions between the bowl and swirl. A CFD model has conducted in KIVA3-VR2 coupled with Chemkin II for detailed chemistry calculations. For optimizing the piston bowl KWICK software has been used. While keeping the squish height and compression ratio constant, thus allowing the bowl volume constant, the KWICK software allow various range of meshes to be generated for optimization of the piston bowl. The control points have selected as the height of the central axis, position of the bottom portion of the bowl, radius of the bowls and height of the lower bowl. The CFD model has validated with experimental results taken from 0.4 L single cylinder engine with 16.5:1 compression ratio. The operating condition has selected to be at medium load with 2000 rpm. The optimalstepped lip model was compared to the conventional model. Results showed that the conventional bowl allowed more soot to be formed due to the fact that this design forces the fuel from second injection to be mixed with the combustion products from the first injection. Stepped desing has allowed the first injection to be targeted to the upper portion of the bowl while the second injection is directed underneath the bowl and thus allowing the fuel to be mixed with the air that is not been a part of first injection, thus resulting with lower soot levels. The analyses also suggested that stepped bowl with a low swirl lowered the fuel consumption by 3 to 3.5% due to having less surface area resulting with reduced amount of wall heat transferred out of the stepped-bowl [7].

Dahlstrom, Andersonn and Tuner have experimentally compared the heat losses of stepped lip and re-entrant combustion chambers in a light duty diesel engine. The experiments were performed on a 2 L diesel engine with 15.8:1 compression ratio. Each cylinder equipped with thermocouples for measuring temperature differences to calculate heat losses to the cylinder head. The operation conditions of the engine include one speed-load test and additional tests in which effects of 4 other parameters have investigated: rail pressure, swirl, EGR and lambda. All experiments have conducted at 1500 rpm and nearly with 10.5 bar IMEPg except in the speed-load tests where the first case was at 2000 rpm and third case with 5.5 bar IMEP. Results from speed-load test implied that the stepped bowl design

reduced the combustion duration while increasing losses to exhaust gas. Rail pressure sweep test showed the heat losses to cylinder head and piston cooling increase with higher rail pressure. The stepped bowl showed shorter combustion durations and increased losses exhaust gas. Swirl sweep tests indicated that the stepped bowl presented higher cylinder head cooling loss, slightly lower exhaust losses and similar piston cooling losses compared with the baseline geometry. The combustion duration was more significantly shortened by higher swirl with the conventional re-entrant bowl than the stepped bowl. EGR sweeps showed reduced heat losses to piston and cylinder head cooling while increasing the exhaust losses. Finally, lambda sweeps showed higher and narrower RoHR with the stepped bowl. Both exhaust, cylinder head and piston cooling losses were higher with the stepped bowl [8].

1.2 Objective of the Thesis

From road vehicles to marine applications, internal combustion engines comprise the biggest usage rate in today's transportation. Due to the fact that these engines use fossil fuels to produce power, as an outcome of incomplete combustions or high combustion temperatures, highly pollutant emissions are released to the atmosphere. These engine-out emissions have been strictly regulated over the years, thus pushing engine manufacturers to produce more environment friendly engines. One solution to meet the emission requirements is to add aftertreatment devices such as particulate filters or catalytic converters to exhaust line in order to decrease the emission levels. Although this method is widely used and has its advantages, it is highly costly and complex to control. Because of these facts engineers had to come with one other alternative method to meet the emission requirements which is to optimize the combustion process happening inside the cylinder. Changing the combustion chamber design is the easiest solution to alter what is happening inside the cylinder. Several design solutions had been tried in the past to decrease the emission levels such as re-entrant or stepped lip combustion chamber. The main idea behind this particular study is to decrease soot emission levels on a single cylinder diesel engine by changing the combustion

chamber design. In order to have an insight on in-cylinder flows, a CFD simulation on ANSYS Forte has been carried out. Finally the models have been experimented and compared with the base combustion chamber of the engine.

1.3 Hypothesis

Decreasing the soot emission levels is made possible by optimizing the combustion chamber. Stepped-lip combustion chamber design can be one way to decrease soot emission due to the fuel separation occurring via the lip radius. Investigation of the effects of the lip radius on air movements by using CFD simulations would give an insight on in-cylinder effects of stepped-lip combustion chamber design. To validate what has been understood from the analyses, an experimental procedure has to be carried out and the emission levels of stepped-lip design has to be compared to the conventional mexican hat combustion chamber in order to have a profound idea.

COMBUSTION CHAMBER DESIGN CI ENGINES

2.1 Working Principle of CI Engines

In reciprocating engines, power is generated from the high-pressure and temperature combustion products and it is transmitted to the driving shafts via the up and down movement of the piston and the crank mechanism. The cyclical movement of the piston is produced via the rotational movement of the crankshaft. When the cylinder volume is at its lower and higher, the movement of the piston comes to rest. These locations are identified as the top dead center and the bottom dead center [9]

In an engine with 4-stroke cycle, in order to generate power, each cylinder has to go through 4 different time steps which equals to 2 revolutions of the crankshaft.

2.1.1 Intake Stroke

The piston movement starts from the top dead center and ends at bottom dead center. In CI engines, the fresh charge air is being drawn into the cylinder. Intake valve timings are adjusted accordingly so that the valve opens just before the stroke begins and closes right after it ends in order to increase the charge air mass [9].

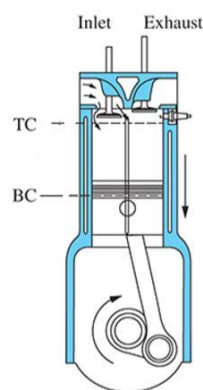


Figure 2.1 Illustration of the intake stroke in CI engines [9]

2.1.2 Compression Stroke

The piston travels from the bottom dead center to the top dead center. The charge air inside the cylinder is being compressed throughout the stroke. Combustion inside the cylinder starts when the piston moves towards the end of the compressions stroke and the pressure inside the cylinder increases rapidly [9].

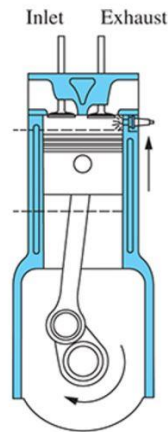


Figure 2.2 Illustration of the compression stroke in CI engines [9]

2.1.3 Expansion Stroke

The piston moves from the top dead center to the bottom dead center due to the forces generated by the high pressure combustion gases. The exhaust valve opens in order to drop the cylinder pressure and initiate the exhaust stroke just before the piston approaches bottom dead center [9].

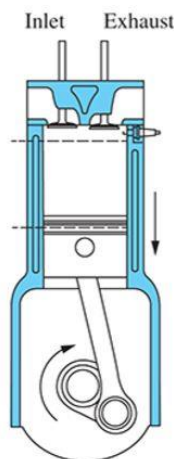


Figure 2.3 Illustration of the expansion stroke in CI engines [9]

2.1.4 Exhaust Stroke

The piston travels from the bottom dead center to the top dead center while the piston is sweeping out the combustion products out of the cylinder [9].

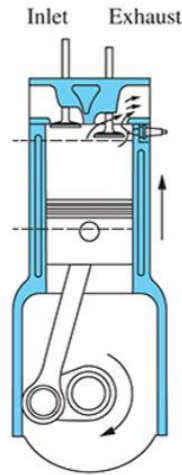


Figure 2.4 Illustration of the exhaust stroke in CI engines [9]

Before investigating the effects of combustion chambers on diesel engine emission, the combustion process throughout the diesel engine must be fully understood. The combustion characteristics of diesel engines strongly depends on the amount of charge air introduced into the cylinder, engine speed, injection strategy and the temperature inside the cylinder.

2.2 Combustion in CI Engines

In diesel engine combustion, near the end of the compression stroke, a certain amount of the injected fuel into the combustion chamber starts to evaporate and mix with the surrounding air. Due to high temperature levels at the end of the compression stroke, the vaporized part of the injected fuel starts burning in a fast rate. The combustion process in diesel engines starts with injecting the fuel inside a combustion chamber and continues until the exhaust stroke begins. The combustion process finishes with the self burning process of the ongoing injection in which the diffused fuel is spread across the turbulently spreading flame zone. The entire process includes complex physical and chemical processes. The combustion process in diesel engines is not homogeneous. The reactions start once the fuel that is injected into hot and pressurized combustion chamber starts to

vaporize. However, in the beginning, no significant increase in pressure is obtained due to low reaction velocities. The significant increase in pressure is seen right after the ignition delay.

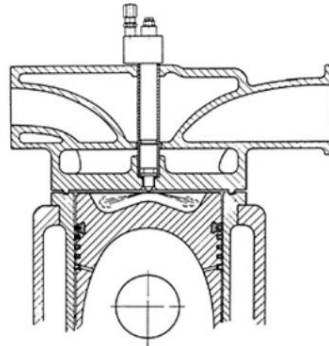


Figure 2.5 Illustration of an injection into a combustion chamber [9]

Figure 2.1 shows a demonstrates a fuel cone entering the combustion chamber. The fuel cone starts spreading across the combustion chamber with an initial angle specified in design procedures of the injector nozzle.

2.2.1 Fuel Spray Behaviour

After the fuel is injected into the cylinder, it goes through several processes in order to generate complete combustion

2.2.1.1 Atomization

This process is identified as the break up of fuel into small sized fuel droplets. Efficient and quicker atomization processes are achieved by smaller fuel drop diameters [10].

2.2.1.2 Vaporization

In CI engines, high temperature levels created during combustion stroke quickly evaporate the small sized liquid fuel droplets. After the evaporation of the first droplet, the circumference is rapidly cooled by evaporative cooling. Vaporization process of fuel droplets are greatly affected by this cooling [10].

2.2.1.3 Mixing

In order to create a combustible mixture, the fuel vapor must mix with the surrounding intake air right after vaporization. The factors that alter the mixing process after vaporization is the velocity of the injected fuel and the turbulence parameters of the intake air such as swirl [10].

2.2.1.4 Self Ignition

Self ignition of the mixture starts shortly after the fuel is injected. The high air temperature inside the cylinder causes secondary reactions to occur such as breaking down the bigger hydrocarbon molecule chains into smaller sizes and a small rate of oxidation. The exothermic reactions release heat to the surroundings and increase the air temperature [10].

2.2.1.5 Combustion

Simultaneous combustions start at the rich zone locations of the fuel jet. Nearly 95% of the fuel is found to be in the vapor state once these local combustions start. The flame fronts generated from the local self ignition zones quickly spread and consume all of the mixture. This phenomenon results in an increase in in-cylinder temperature and pressure. The increased temperature levels cause a reduction in vaporization time and increase the local self ignition points to increase the combustion process [10].

2.2.2 Combustion Phases in Diesel Engines

The phases of the injected fuel and the combustion process is explained in this chapter. In diesel engines, the combustion process happens in 4 separate phases. These phases can be classified as: ignition delay, pre-mixed combustion, diffusion controlled combustion and late combustion.

2.2.2.1 Ignition Delay

The time interval between the start of injection and the start of combustion is identified as the ignition delay. The fuel continues to be injected and vaporized throughout this combustion process. Ignition delay is a function of vaporization ratio and the parameters that affect chemical reactions. The fuel has to be

separated into small droplets, must be vaporized and mixed with the surrounding air before certain reactions start. The main parameters that effect the ignition delay are the ambient temperature, ambient pressure, injection timing, total injected mass, engine speed, vorticity ratio and the properties of the fuel [11].

2.2.2.2 Pre-Mixed Combustion

Spontaneous burning of the fuel air mixture and the time passed right after this phenomena is called pre-mixed combustion. The most important parameter that effects this phase of the combustion process is the ignition delay. The amount of burned fuel right after the ignition delay depends on the fuel properties, injection parameters, in-cylinder flow characteristics, in-cylinder pressure and temperature and the ignition delay. The fuel starts the burn spontaneously once the ignition strats. During this period the heat release rate per crankshaft degree reaches its maximum. Long ingnition delay periods increases the amount of fuel entered into the combustion chamber during this phase. With an instant increase in pressure major maximum pressure levels are obtained and a characteristic sound occurs. This operating conditions can lead to mechanical failures and in order to prevent this situation, strategies like delay in injection timing, introducing a little amount of exhaust gas into the cylinder or heating the intake air can be tried. However this strategies can lead up to poor performance and emission characteristics [11].

2.2.2.3 Diffusion Controlled Combustion

Right after the pre-mixed combustion phase, the fuel continues to be injected into the burning zone and the combustion products. This phase of the diesel combustion process is defined as diffusion controlled combustion. The burning rate is controlled with the mixing rate of fuel vapor with surrounding air. However, in cold start conditions, the droplet vaporization becomes the most important factor that controls burning rate.

The atomization of liquid fuel, vaporization, mixing process of fuel vapor and intake air and the chemical reactions before burning are all occuring in this phase of the diesel combustion. The resulting flame during this process is extremly bright due to creation of carbon particles [11].

2.2.2.4 Late Stage Combustion

During expansion process, the heat release still continues with a small rate caused by a fraction of unburned fuel or energy release from combustion products of rich mixtures. The kinetics of post combustion slows down throughout the expansion process due to the drops on in-cylinder temperature [11].

The total amount of heat release per crank angle degree throughout the diesel engine combustion process is shown in the Figure 2.6.

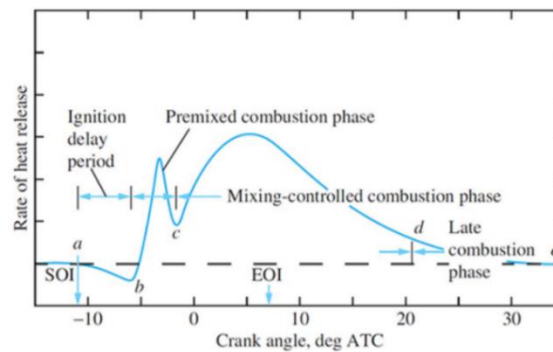


Figure 2.6 Total heat release rates in a diesel combustion [9]

2.3 Pollutant Formation in Diesel Engines

In internal combustion engines, the mixing process of intake air and the injected fuel inside the combustion chamber and, the chemical reactions of this mixing results in combustion products. These combustion products may include harmful components induced by either non-complete burning processes or high temperatures such as soot or NO_x emissions. Over the years there were many strict regulations implemented to restrict this emissions which led engineers to come up with alternative solutions [9]. Nowadays, many aftertreatment devices are assembled on an engine in order to meet the required emission levels but the cost and complex control mechanisms of this devices pushed engineers to solve this problems in a more cost effective and easily implemented way such as combustion chamber designs. The geometrical shape of the combustion chamber can alter the air flow structures or can be effective with fuel targetting. All of this aspects can result in different temperature or velocity fields in a combustion system which can effect the in-cylinder pollutant formations. Thus, before designing a combustion

chamber system, the in-cylinder pollutant formation mechanisms must be fully understood.

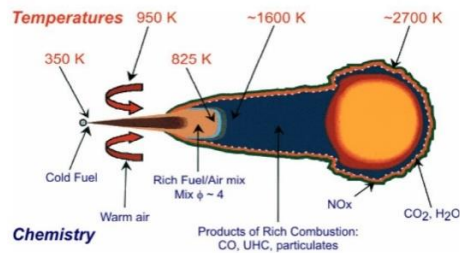
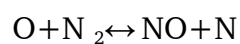
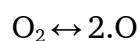


Figure 2.7 Temperature distribution and emission formation on a fuel spray [12]

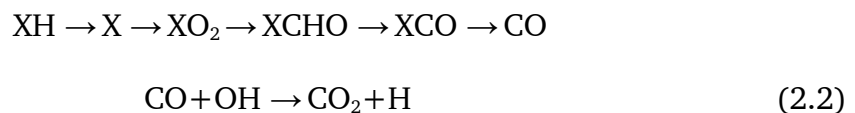
2.3.1 NO_x Emissions

Almost 79% of the air contains nitrogen which is the main source of NO_x emissions in diesel combustion. Although there are other formations of NO_x emissions, only NO and NO₂ levels are considerably high. There are 2 main formation mechanisms for NO and NO₂ emissions. The first formation mechanism is the thermal binding of O₂ and N₂ inside the combustion air at high temperatures. The second formation mechanism is the reaction between the atmospheric O₂ and the nitrogen compounds in the fuel. Due to the fact that the combustion durations are very low, the amount of time to oxidize NO into NO₂ is restricted, thus the products of these NO_x formation mechanisms are mainly NO. NO₂ forms at low temperature levels and the main reason behind the formation of photochemical smoke is the oxidation of NO into NO₂ in the atmosphere. NO is formed behind flame front where the nitrogen and oxygen atoms are found with burned gases in high temperatures. With higher temperatures, formation rate NO increases. The reactions that create NO slows down in the expansion process since combustion gases start to cool down and the NO levels stay above the equilibrium region. The best way to describe the NO formation is the Zeldovich mechanism which is assumed to happen in stoichiometry and depends on thermal equilibrium. The Zeldovich reactions are given below [11]



2.3.2 Carbon Monoxide (CO) Emissions

CO emission levels in diesel engines are considerably lower compared to spark ignition engines and only increases when the combustion process reaches the soot limit. CO emission are linked with excess air ratio. CO emissions occur as a result of incomplete combustion. The mechanism that controls CO formation is chemically and kinetically controlled. In pre-mixed hydrocarbon-air flames, CO concentration peaks at the flame zone. The CO concentration levels are higher than the equilibrium levels when the fuel is believed to be burning adiabatically. The CO₂ formation mechanism is shown below. The X in the equations represents hydrocarbon bases [11].



2.3.3 Hydrocarbon (HC) Emissions

Hydrocarbons are considered organic emissions. The main reason behind HC emission formation is the incomplete combustion process. With high air-fuel ratios, the combustion temperatures will decrease and results in increased HC emission levels. With lower air-fuel ratios, due to the insufficient amount of oxygen, the HC emission levels will increase. The main events that triggers the HC emission formations are are depletion on air-fuel ratio, insufficient mixing, misfire, engine oil absorption and crevice mechanism. [11].

2.3.4 Soot Emissions

Soot emissions are defined as the mass of nonabsolute carbon particles which results from the incomplete combustion processes. The H₂ molecules inside the liquid fuel droplets starts to go through chemical reactions while the unburned C particles which did not found sufficient oxygen are thrown out of the the cylinder in soot particle form. Although the reasons behind soot formation may vary depending on the fuel type, the main reason is insufficient mixing of fuel and air. Additionally, vaporizing ability of the liquid fuel can be a reason behind soot formation as well. Soot formation inside the cylinder begins in diffusion controlled

combustion phase, increases throughout the injection process and reaches its maximum level once the injection ends. The soot level starts decreasing with oxidation although the oxidation slows down as the combustion temperatures decrease [11].

2.3.5 Soot-NO_x Trade-off

The balance between the formation mechanisms of soot and NO_x emission are very critical in order to control pollutant formation on a diesel engine. The theory behind the problem lies within the opposite behaviour of soot and NO_x emissions. The control methods used to decrease NO_x emissions end up increasing soot emission levels. The most effective method to decrease NO_x emissions is to avoid combustion temperatures to be above 2000-2200 °K. Injection parameters, injector design parameters (such as cone angle or number of holes), combustion chamber designs and air flow characteristics must be adjusted into the targeted soot-NO_x trade-off levels [11].

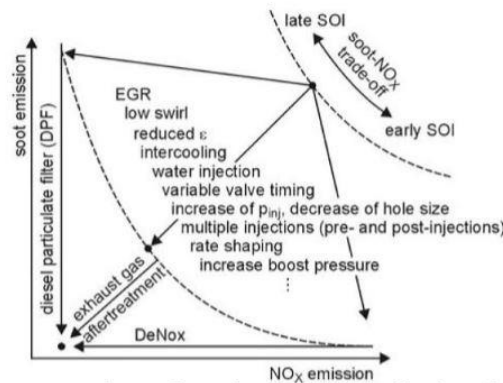


Figure 2.8 Demonstration of soot-NO_x trade-off [13]

2.4 Combustion System Design in Diesel Engines

The geometrical shape of the combustion chamber is an important factor for altering in-cylinder air motions alongside other engine design parameters such as compression ratio or cylinder displacement. The most important factor to consider while designing a combustion chamber is the compression ratio due its effects on peak cylinder pressure, air-fuel ratio, mechanical and thermodynamic efficiency, emissions and fuel consumption.

Main factors to take into account when designing a combustion chamber can be summarized as;

1. The compression ratio of the engine must be selected in such manner that the cold start capability of the engine and the peak cylinder pressure is acceptable. Lowering the compression ratio results in decreased thermodynamic efficiency and increase in ignition delay.
2. The combustion chamber design must be in sync with the injection system and inlet swirl achieved by intake port design for good mixing. The geometrical shape of the combustion chamber alters such functions as swirl and vortex generation in the bowl, turbulence of in-cylinder flow and the wall impingement.
3. Heat losses from the combustion system must be minimized. In order to achieve this, a low surface-to-volume ratio is preferred.
4. The geometric shape of the bowl directly affects the metal temperatures of the piston. Thus the thermal fatigue factors must be taken into consideration while designing a combustion chamber.
5. Final parameter to consider is the combustion noise which may be optimized by turbocharging or injection strategies.

Combustion chamber design parameters are highly dependent on engine design parameters. Therefore, when designing a chamber, all kinds of engine parameters and air flow parameters must be kept in mind [14].

2.4.1 Engine Parameters

2.4.1.1 Cylinder Displacement

Engine displacement is the most important factor for engine system design. Fuel consumption levels and peak power density targets alongside power and torque requirements of the vehicle, can define the cylinder displacement value for an engine. Although high power and torque levels are always beneficial, there is a certain trade-off that engineers must be aware of. High power and torque levels are always linked with a more rigid cylinder block and cylinder head design, more intimate charging and more efficient aftertreatment solutions [14].

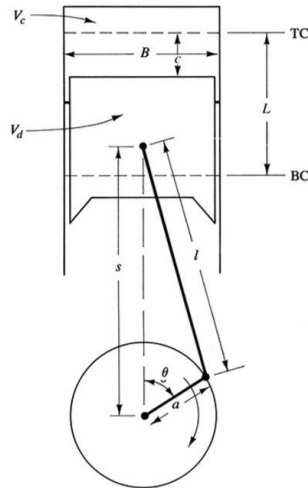


Figure 2.9 Geometric view of an cylinder piston mechanism [9]

The total displacement of an engine V_{engine} can be calculated as:

$$V_{engine} = n \frac{\pi B^2}{4} L \quad (2.3)$$

with B is the bore diameter, L is the stroke length and n is the number of cylinders.

Engines which have lower cylinder displacement values and high power densities mostly operate at high load profiles in which the losses to friction and heat are smaller. Engines with higher cylinder displacement value are beneficial for employing lower boost levels, injection pressures and swirl ratios.

2.4.1.2 Compression Ratio

Compression ratio can be defined as the sum of displaced volume and clearance volume divided by the clearance volume.

$$r_c = \frac{\text{maximum cylinder volume}}{\text{minimum cylinder volume}} \quad (2.4)$$

Increasing the compression ratio will result in increasing thermal efficiency. However there are some there-offs that would result with high compression ratios;

1. To achieve allowable peak cylinder pressures or engine-out emissions, retarding the combustion event must be necessary in engines with high compression ratios.

2. With high compression ratios, higher compression pressures are achieved. The increase in pressure will result in increase in piston ring and journal bearing friction.
3. When increasing the compression ratio, an increase in surface area-to-volume ratio occurs while the piston approaches top dead center. This would result in increased heat losses to the piston and cylinder head.
4. Increasing the compression ratio increases the difficulty of utilizing the air. The ratio of the volume inside the bowl to the total volume at top dead center is called the k-factor. This ratio must be optimized accordingly to achieve better air utilization, higher torque and power at high loads hence higher efficiency at high loads [14].

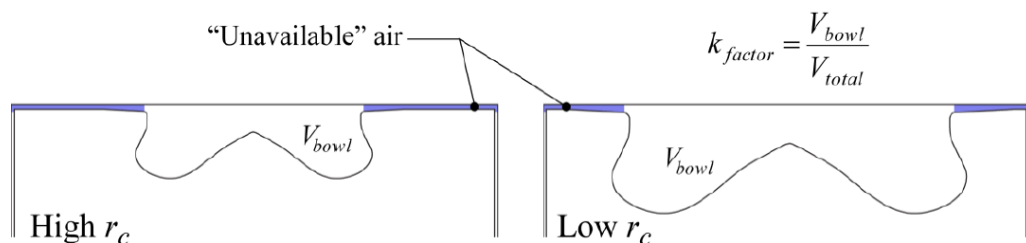


Figure 2.10 Illustration of k-factor for both high and low compression ratios [14]

However, there are certain advantages that comes with increasing the compression ratio;

1. Increasing the compression ratio shortens the ignition delay by increasing compression temperatures. Additionally increased compression ratio can result in better engine out HC and CO emissions.
2. Combustion noise may also be decreased by shorter ignition delay.
3. Increased compression ratio results in lower exhaust gas temperatures and better tolerance to higher BMEP values.
4. Cold start characteristics of the engine may improve with high compression ratios

On the other hand, there are some benefits of having a low compression ratio value:

1. Lower compression ratio values will result in increase in specific power.
2. Lowering compression ratios would reduce the compression and peak combustion pressures which would result with decrease in NO_x formations and increase in ignition delay. An increase in ignition delay would cause more fuel-air premixing which lowers soot formation.
3. A decrease in exhaust gas temperatures can be achieved by lowering the compression ratio which will result in more energy extraction by the turbocharger. Thus allowing higher boost levels at low speeds.
4. Slower cooling rates in expansion can be obtained by low compression ratios which provides more time for soot oxidation and other unburned particles [14]

2.4.1.3 Bore-to-Stroke Ratio

Bore-to-stroke ratio in diesel engines are typically near 0,9. Besides the fact that bore-to-stroke ratio clearly impacts the packaging of the engine, it also has significant effect on efficiency and combustion system design. Using large bore-to-stroke ratio has many advantages:

1. Friction is the main parameter which is influenced by bore-to-stroke ratio. Piston assembly frictions scales are related to bore-to-stroke ratio and having short stroke engines will result in lower friction.
2. Reduced piston speeds are found in large bore-to-stroke engines thus increased crankshaft rotation speeds and increased peak power levels are obtained.
3. Larger inlet valve areas are implemented in large bore-to-stroke engines which allows higher charge air flow rates resulting in increased engine power and torque density.
4. Wider bowl designs can be obtained with engines having larger bores which could be beneficial for reduced risk of liquid fuel wetting the bowl walls during cold start conditions when vaporization is impeded.

Disadvantages of having a large bore-to-stroke ratio is given below:

1. Having large bore-to-stroke ratios would decrease the k-factor which results in less efficient air utilization.
2. Turbulent velocity fluctuations are reduced in engines with large bore-to-stroke ratios therefore increase in turbulent mixing times are expected which results in slower combustion rates.

To summarize, engines with large bore-to-stroke ratios are suitable for increased power density applications while engines with small bore-to-stroke ratios are used for higher engine efficiency [14].

2.4.1.4 Connecting Rod to Crank Radius Ratio

Kinematics of the piston are highly influenced by the ratio of the connecting rod length to the crankshaft radius. Besides the fact that this parameter can effect the friction levels, balancing problems, packaging volumes and manufacturing costs, it can also effect the engine efficiency. Engines with larger connecting rod to crank radius ratio has slower piston motion near top dead center, allowing more time for heat release and also more time for heat transfer [14].

2.4.2 Piston Bowl Design Parameters

The geometrical shape of the combustion chamber plays an important role in altering the in cylinder fuel and air motion to support the combustion process. Thus, effecting both engine efficiency and emission characteristics. Because of the fact that there are complex relations between the chamber geometry, in cylinder air flow and fuel injection parameters, it is hard so state certain laws that apply to all engines [14].

2.4.2.1 Axisymmetry

In order to promote efficient air utilization and emission characteristics, axisymmetry play an important role. Axisymmetry has a crucial role in implementation of 4-valve cylinder head designs with central piston bowls and injectors that are located through the cylinder axis. One major factor that effects

the combustion chamber symmetry is valve pockets on top of the piston even though it significantly improves the k-factor [14]

2.4.2.2 Piston Bowl Diameter

Many computational works suggested that the bowl diameter is the most important factor in piston design which is directly affecting the combustion performance. Here are the benefits that would come with increasing the piston bowl diameter.

1. Longer free spray lengths are provided with large bowls which is beneficial for higher power density usages since engines with higher power densities require larger nozzle diameters and longer spray prolongation lengths.
2. Wide bowl applications are suitable for low compression ratio designs because of the fact that increased spray penetration due to lower ambient density.
3. Due to the fact that wider bowl designs improve the k-factor, more favorable surface-to-volume ratios are achieved, resulting in reduced heat load on the piston.
4. More advanced injection and spray targeting strategies can be obtained with wider bowls which will prevent oil dilution [14].

2.4.2.3 Bowl Re-entrancy

Piston re-entrancy is important due to promoting the amplification of the swirl velocity while the air charge is compressed into the bowl. It also highly impacts the strength of the squish flow. Therefore, optimizing piston re-entrancy affects turbulence structures and air fuel mixing levels within the bowl. Additionally, the kinetic energy of the fuel spray is preserved later it contacts the piston wall, thus channelling the flow to the center of the cylinder. This situation prevents the stagnation of rich mixtures at the bottom of the wall. The swirl flow during expansion is retained thus preventing the spread of burning liquid into the squish region. Finally, more re-entrant bowls tend to have higher piston rim temperatures and can decrease ignition delay, resulting with lower combustion noise levels and improved cold-start emission levels.

On the other hand, lower re-entrancy promotes robustness and beneficial for variable injection strategies [14].

2.4.2.4 Squish Height

The squish height on a piston design must be kept as small as possible. Soot emission, HC emissions and CO emissions are decreased with lower squish height but too small of levels of squish height would result in severe manufacturing problems. Additionally, through high heat loss levels with smaller squish heights, fuel consumption levels can be minimized [14].

2.4.2.5 Bowl Pip Geometry

The central protrusion on the bowl floor referred to as the bowl pip. This section of the combustion chamber is where the velocity profiles of air and fuel and mixing levels are decreased thus creating efficient mixtures becomes harder. The advantages of having a bowl pip can be summarized as;

1. Inward deflected fuel jets by the bowl walls are, directed upwards thus stagnation of rich mixtures are avoided.
2. Turbulence levels within the bowl are increased hence better mixing rates are achieved [14].

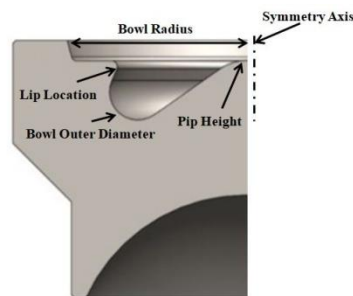


Figure 2.11 Demonstration of piston combustion chamber design parameters

2.4.3.6 Bowl Lip Shape

Because of turbulence generated by the contrary squish flow caused by a small radius at the upper lip side of the combustion chamber, bowls with lip radiuses are beneficial for decreasing soot emission levels. Piston durability issues limit the size of the lip radius. Dissipation of the fuel spray inside the piston bowl and the

flow structure strengths are affected by the spray angle which affects the chamber lip and the radius around the lip. Illustration of the bowl lip shape is shown below [14].

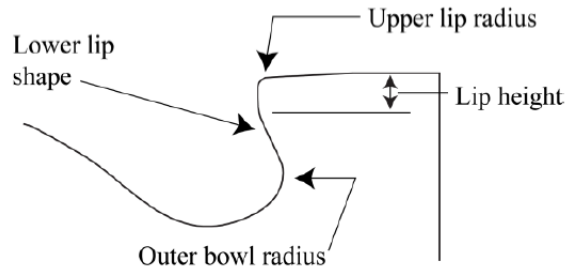


Figure 2.12 Illustration of the lip radius on a bowl [14]

2.4.3 Air Flow Parameters

It is stated before that the interactions between injection strategies, air motion and the combustion chamber geometry must all be taken into account while designing the chamber. In this section the air flow parameters and injection strategies are summarized.

2.4.3.1 Swirl Flow

The organized rotation of the inlet air around the cylinder axis is referred to as swirl and is generated by introducing the air into the cylinder with an initial angular momentum. Although friction during engine cycles causes swirl to decay, the air motion continues throughout the compression, ignition and expansion processes. Throughout the compression stroke, the rotational movement of the introduced air is strongly modified by the combustion chamber design in the bowl. Swirl is used as a promoter of more rapid mixing between the intake air and the fuel. In an engine, swirl ratio (R_s) is defined as the angular velocity of the intake air (ω_s) divided by the angular rotational speed of the crankshaft [9].

$$R_s = \frac{\omega_s}{2\pi N} \quad (2.5)$$

In order to generate swirl during intake, there are two general methods to apply on an engine. The first method is to introduce the air into the cylinder tangentially

toward the cylinder wall in which to flow is deflected sideways and downward. The second method to generate swirl is via intake port designs where the flow is forced to rotate around the valve axis, thus gaining nonuniform flow distribution around the valve circumference, before the air is introduced into the cylinder.

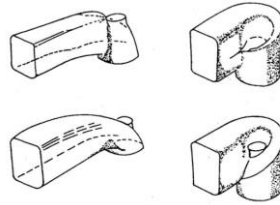


Figure 2.13 Various types of inlet port designs [9]

2.4.3.2 Squish Flow

Squish is a radially inward gas motion that happens at the end of the compression stroke when the piston top surface and cylinder head are close. The charge air is pushed inside the bowl and thorough mixing of air and fuel is promoted thus increasing the efficiency of the combustion [9].

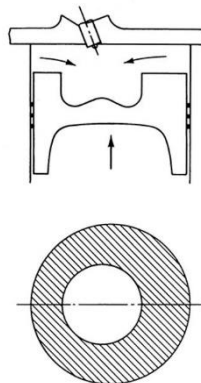


Figure 2.14 Squish flow on a direct injection combustion chamber [9]

Squish velocities can be calculated with ignoring the gas motion mechanisms, friction losses, heat losses and leakage past the piston ring. For a combustion chamber design with a bowl-in design, the squish velocities (v_{sq}) are defined as;

$$\frac{v_{sq}}{S_p} = \frac{D_b}{4Z} \left[\left(\frac{B}{D_B} \right)^2 - 1 \right] \frac{V_{bowl}}{A_c Z + V_{bowl}} \quad (2.6)$$

where V_{bowl} is the piston bowl volume, D_b is the bowl diameter, A_c is the cross sectional area of the cylinder, S_p is the piston speed and Z is the distance between the top of the piston and the cylinder head [9].

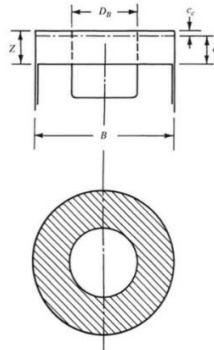


Figure 2.15 Demonstration of the measures in order to calculate squish velocities [9]

2.4.3.3 Tumble Flow

When the piston approaches near top dead center, the secondary rotational flow due to squish flows is identified as tumble flow. Tumble flow on a combustion system happens around the circumferential axis near the outer side of the piston bowl edge. Demonstration of a tumble flow is given below

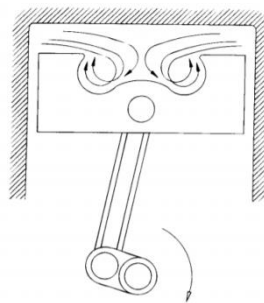


Figure 2.16 Tumble flow in a combustion chamber [10]

2.4.4 Fuel Injection Parameters

In an diesel engine, the fuel is brought into the cylinder via a nozzle which has a large pressure differential around the orifice. Fuel injection pressure can vary between 200 bar up to 3000 bar depending on combustion system implemented in the engine. The large pressure difference around the nozzle orifice is necessary in order to force the fuel into the chamber with high velocity levels. The main

reasons behind this is to atomizing the fuel in order to achieve rapid evaporation and for complete utilization of the intake air. The fuel injection system of an engine is obligated with leveling the quantity of the fuel in any engine operating condition and injecting the fuel into the combustion chamber at the right time in the cycle with optimized spray structure.

2.4.4.1 Spray Structure

Once the liquid fuel jet starts to leave the injector nozzle, it becomes turbulent and spreads out through the combustion chamber while mixing with the charge air inside the cylinder. Near the nozzle surroundings, the fuel jet breaks up into small droplets. The break-up length of the fuel is defined as the disintegration length of liquid fuel while it is moving through the combustion chamber. While the fuel moves further away from the injector nozzle, increased air mass within the spray is obtained, the spray flow becomes more disorientated and its velocity is decreased.

As the mixing process with air continues, the fuel droplets start to evaporize, although the end of the fuel cone still moves across the combustion chamber at a slower rate [9].

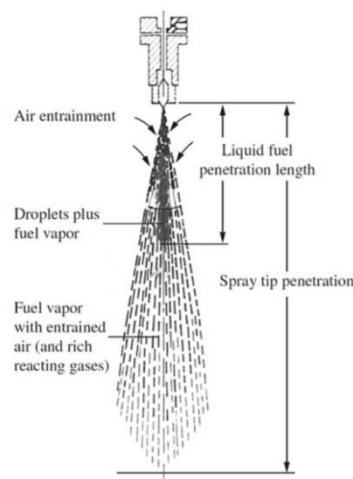


Figure 2.17 Fuel spray structure [9]

2.4.4.2 Atomization Process

During the diesel engine injection process, a cone shaped structure is formed at nozzle tip. This phenomena is referred as the atomization breakup regime, and small droplets are produced at smaller sizes than the nozzle diameter. The unstable increase in surface waves causes the break-up at low jet velocities and the droplet sizes are larger. With increased velocities, the motions of air and the jet increase the surface tension force which results in droplet sizes of the order of the diameter of the fuel jet. This situation is called the first wind-induced break-up regime. As the jet velocity increases, a break-up identified with the divergence of the fuel jet occurs. During the second wind induced break-up, the kinematics between the surrounding air and the fuel excites the growth of waves which have short wave lengths thus resulting with droplet sizes smaller than the fuel jet diameter. Aerodynamic increases between the liquid\gas interface causes the droplet sizes to be even more smaller than the fuel jet diameter as the velocities increase even further [9].

2.4.4.3 Spray Penetration

Another important factor that effects fuel-air mixing rate is the spray penetration along the combustion chamber. The speed and the extend of the fuel spray has a direct effect on air utilization. With engines which have hot walls and higher swirl rates, it is beneficial to have fuel impingement on the walls. With engines which have multi-spray injection systems, over penetration of the fuel may end up with impingements on the cool surfaces and may result with decreased mixing rates and increased unburned combustion products. However smaller fuel spray penetration lengths would decrease the utilization of the air on the periphery since fuel spray does not contact the walls of the combustion chamber [9].

2.4.4.4 Droplet Size Distribution

In order to evaporate the liquid fuel, breaking the fuel down into small size droplets is critical for achieving a large surface area. Drop sizes across the spray envelope strongly depends on injection, fuel and air parameters. The variations of injection pressures, nozzle orifice areas or injection rates could alter the size

distribution at any given location inside the combustion chamber. Since the atomization process differs from the spray core to the spray edge and the trajectories of fuel droplets vary with different initial velocities and different locations in the spray envelope, the size of fuel droplets is considered variable along the specific positions of the fuel spray [9].

2.4.4.5 Spray Evaporation

The atomized fuel spray with small droplets near the nozzle area, must be evaporized before it could mix with the charge air and burn. In a standard diesel engine at end-of-compression there three main deciding factors that effects fuel evaporation:

1. Aerodynamic drag induced deceleration
2. Heat transfer from the ambient air
3. Total transferred mass of vapor fuel extracted from the fuel droplet

The rate of evaporation and the vapor pressure increases due to increased droplet temperature that is caused by heat transfer out of the hot surrounding ambient air. An increase in the mass transfer rate of the fuel vapor would result in decrease in drop temperature. As the velocity of the drop decreases, a decrease in the convective heat transfer coefficient between the drop and the surrounding air is obtained as a result.

Optimizing the fuel injection strategy for diesel combustion system is critical for meeting the targeted power density levels and matching the bowl shape with the swirl characteristics of the engine. The flow capacity of the injector and the maximum injection pressure have to be selected properly in order to have enough fuel to meet the power necessities of the engine. Number of nozzle holes on the injector, diameter of the nozzle holes and the nozzle hole discharge coefficient are the parameters that effect the flow capacity. Throughout overall injection duration, injector needle disclosure and inclosure specifications will also have an affect on the level of fuel being brought to the combustion chamber. The nozzle hole diameter and the number of holes are highly dependent on how the fuel cone is interacting with the air motion inside the cylinder and the combustion chamber

geometry. Higher swirl levels usually applied with injectors with less holes and the spray targeting strategies are directly affected by the interactions between the piston combustion chamber geometry, and the fuel cone which is dependent on the injector protrusion and the fuel included angle but it is worth mentioning that increased injector protrusion levels may increase the temperature at the nozzle tip thus resulting with increased deposit formations inside the nozzle [9].

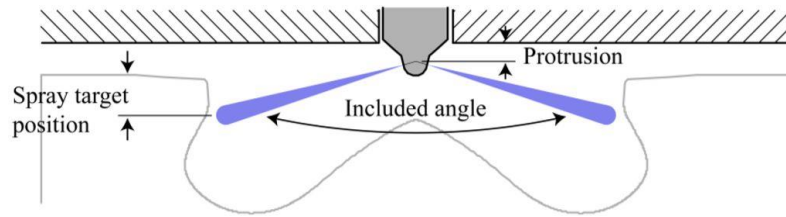


Figure 2.18 Illustration of a spray targeting method [14]

2.4.4.6 Fuel Targeting and Piston Bowl Optimization

Aiming the fuel cone on a combustion system is implemented as a strategy to achieve better fuel-air mixing by utilizing the air charge inside the cylinder as much as possible thus resulting in better soot emission level performance. Therefore, targeting the fuel to a specific region in a chamber via changing the nozzle parameters or fuel injection advance gains significant importance.

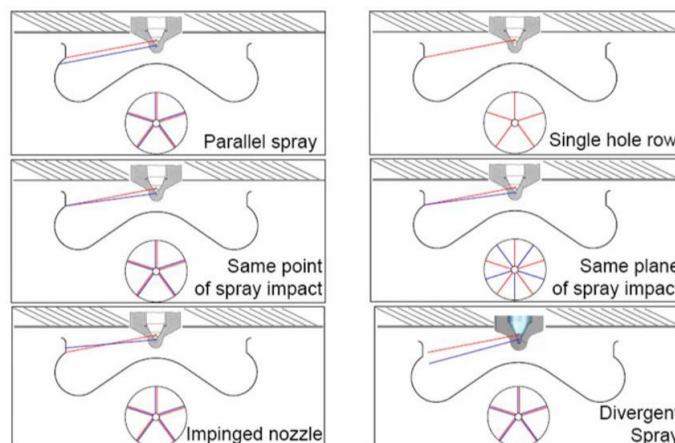


Figure 2.19 Various options for fuel targeting and nozzle configurations [15]

Recently Volvo company has developed a combustion chamber design where the fuel cone is separated radially clockwise and counter clockwise. There several

other combustion chamber designs investigated in the literature all uses the same fuel cone separation idea.



Figure 2.20 Volvo wave piston model [16]

In the wave piston model created by Volvo company, the fuel is targeted between two longitudinal protrusions, creating two lateral clockwise and counter clockwise flow patterns which follow the protrusion surface and the mixture is directed towards to the center of the cylinder. Thus, achieving better fuel-air mixing by optimizing the geometrical shape of the combustion chamber.

In another study, Li, Zhou, Su and Chen have used the same fuel separation idea by using longitudinal protrusions. In this design fuel cone is targeted in the center of the protrusion tip radius which creates two lateral swirl profiles thus resulting in considerable levels of soot reduction [17].



Figure 2.21 Lateral swirl combustion chamber [17]

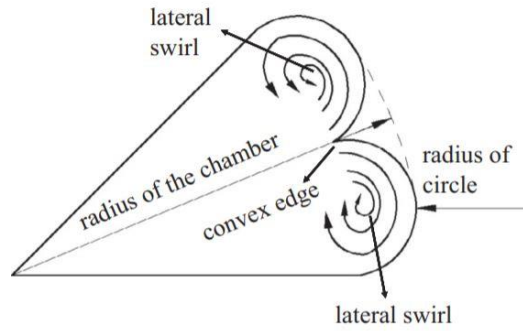


Figure 2.22 Lateral swirl formation mechanisms [17]

2.5 Types of Combustion Chambers

Diesel engine combustion systems are generally separated into two categories: direct injection combustion chambers in which the fuel targeted directly into the combustion chamber and indirect combustion chambers where the fuel goes through a prechamber which is divided from the main combustion chamber. These combustion systems have different chamber geometries, air-flow and fuel injection strategies [9].

2.5.1 Direct Injection Combustion Chambers

Direct injection combustion chambers are the systems where the entire volume is located in the main cylinder and the fuel is injected directly into the combustion chamber. This type of usage is beneficial due to less contact with coolant and increased fuel economy levels [9].

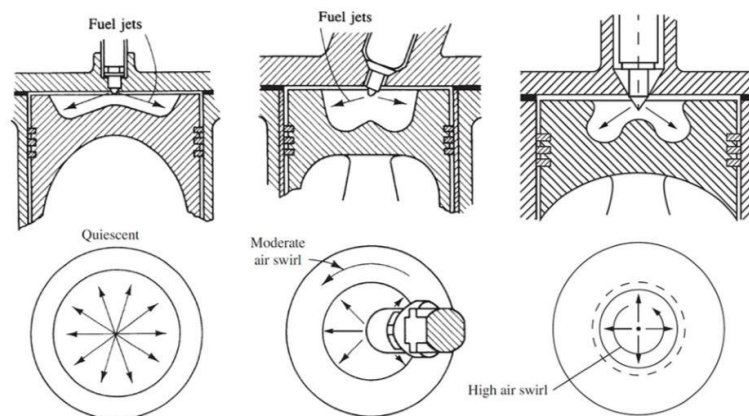


Figure 2.23 Various types of direct injection combustion chambers [9]

As shown in Figure 2.5.1, direct injection combustion chambers can be used with various geometrical shapes, swirl levels and injection strategies. In larger size engines in which the mixing rates requirements are not the primary concern, more quiescent combustion chambers that are shown on the left are being used. In this types of combustion chambers, elevating air movement inside the cylinder is not required. Increased levels of swirl are being used once the combustion chamber size gets smaller due to achieving faster mixing rates. The two other combustion chambers shown in the Figure 2.5.1, illustrates the chambers with increased levels of swirl where the air is pushed into a bowl-in-type combustion chamber. The combustion chamber in the middle belongs to a medium size direct injection engine with a centrally located injector. The main purpose of this combustion chamber is to minimize the amount of fuel which impinges on the piston bowl. And finally, the chamber design on the left belongs to a small, high speed direct injection engine which uses higher levels of swirl with a re-entrant combustion chamber design [9].

2.5.2 Indirect Injection Combustion Chambers

For small, high speed diesel engines, usage of air swirl is not a sufficient way to provide more enhanced air-fuel mixing. Instead, indirect injection systems are implemented where the air charge is mixed with the fuel in a separate combustion chamber during compression stroke.

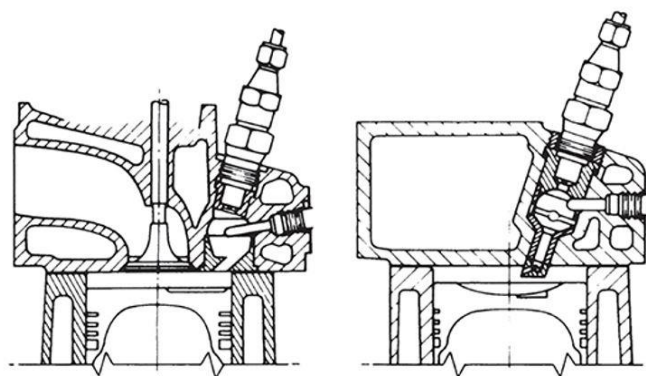


Figure 2.24 Various indirect injection combustion chamber designs

Swirl chamber and prechamber systems are the two widely used indirect injection combustion chambers. The charger air is pushed into the precombustion chamber

through orifices during compression stroke thus creating a vigorous flow inside the chamber. In swirl chamber systems, the passage is in such shape that the air flow inside the prechamber has fast rotational speed. Then the fuel is injected into the separate combustion chamber at lower injection pressures compared to direct injection systems. The increased pressure in the separated combustion chamber forces the gases into the main combustion chamber where the fuel is mixed with the air inside the main combustion chamber. A glow plug in indirect injection systems, shown in Figure 2.5.2, is used as a cold start aid [9].

COMPUTATIONAL FLUID DYNAMICS SIMULATIONS

In order to understand fluid mechanics of internal combustion engines, computational fluid dynamics (CFD) tools are proven to be really useful. Engineers became capable to simulate complex fluid dynamics calculations such as laws of mass, momentum and energy conservation equations with turbulence models and fuel chemistries in a short amount of time compared to analytical and experimental methods. This results in obtaining large amount information with a cost effective solutions in short cycles. Results obtained from repeatable 3D CFD tools help engineers to optimize port, valve or combustion chamber designs. Additionally, situations with high temperatures and dangerous environments which is hard to experiment, can be simulated easily. Although CFD tools can provide quick insights, there are several challenges that brings complexities such as creating meshes for moving and non-moving parts of the engine, defining valve motions or post-processing the datas obtained from 3D CFD analyses.

Cold flow simulations are transient analyses which are used in order to capture air movement inside a combustion chamber with the absence of chemical reactions. This type of simulations are able to predict the swirl or squish flow formation inside the cylinder [referans]. Also, mixing characteristics with the injected fuel can be predicted with the formations of the vortices while the piston approaches top dead center [17].

3.1 Mathematical Background

The research field of fluid dynamics intensively studies the motions of atoms with large quantities. Also, in order to define a continuum of this atoms, the fluid density is supposed to be sufficient. This means, for the smallest sized element, there will be enough amount of particles in which the velocity and kinetic energy calculations would still be applicable. Important parameters in order to understand the fluid behaviour such as velocity, density, pressure etc. are all made possible to calculate this way [18].

The laws that define the dynamic behaviour of a fluid is given below:

- Conservation of mass
- Conservation of momentum
- Conservation of energy

3.1.1 Conservation of Mass

Mass conservation or continuity equations states that mass cannot be created or destroyed. It can be understood from this statement that any variation of mass would imply a shift of fluid particles.

3D mass conservation equation for a compressible fluid is given as below;

$$\frac{\partial \rho}{\partial t} + \nabla(\rho \mathbf{u}) = 0 \quad (3.1)$$

Where the first term stands for mass per unit volume and the second term is net mass flow out of an element with ρ standing for density and \mathbf{u} is the velocity vector [18].

3.1.2 Conservation of Momentum

It is stated in the Newton's Second Law that the change rate of momentum in a fluid is equal to all of the forces applied to the fluid.

Conservation equations for momentum for a compressible fluid in x, y, z directions are given as below;

$$\frac{\partial}{\partial t}(\rho u) + \nabla(\rho u \mathbf{u}) = -\frac{\partial p}{\partial x} + \nabla(\mu \cdot \text{grad } u) + S_{M_x} \quad (3.2)$$

$$\frac{\partial}{\partial t}(\rho v) + \nabla(\rho v \mathbf{u}) = -\frac{\partial p}{\partial y} + \nabla(\mu \cdot \text{grad } v) + S_{M_y} \quad (3.3)$$

$$\frac{\partial}{\partial t}(\rho w) + \nabla(\rho w \mathbf{u}) = \frac{\partial p}{\partial z} + \nabla(\mu \cdot \text{grad } w) + S_{M_z} \quad (3.3)$$

where S_M stands for the momentum source [18].

3.1.3 Conservation of Energy:

The first law of thermodynamics defines the conservation of energy equations. It is stated in the law that the change rate of energy of a fluid is equal to the added heat rate and the rate of work applied on the fluid.

Energy conservation equations for a compressible flow is given as below;

$$\frac{\partial}{\partial t}(\rho i) + \nabla(\rho i \mathbf{u}) = -p \cdot \nabla \mathbf{u} + \nabla(k \cdot \text{grad } T) + \varphi + S_i \quad (3.4)$$

where φ stands for dissipation function, T is temperature and i is total energy [18].

3.1.4 Turbulence Model

Understanding the turbulence mechanism is important for systems with high velocity profiles. In an internal combustion engine, the intake air gains high velocities and turbulence levels while it passes through the inlet valves. The turbulent movement of the air continues throughout the compression process while the piston approaches top dead center. Heat transfer levels, mixing of fuel-air and combustion structures are all affected by turbulence levels inside the cylinder.

For better understanding the turbulence characteristics, mathematical turbulence models are required and selecting the suitable turbulence model is highly important. The RNG k - ε turbulence model is mostly used in internal combustion engine applications due more accurate calculations of vorticities inside the combustion chamber [referans], therefore, it is selected for this study. The equations for RNG k - ε are given below;

$$\frac{\partial}{\partial t}(\rho k) + \nabla(\rho k \mathbf{u}) = \nabla[\alpha_k \cdot \mu_{eff} \cdot \text{grad } \varepsilon] + \tau_{ij} \cdot S_{ij} - \rho \varepsilon \quad (3.5)$$

$$\frac{\partial}{\partial t}(\rho \varepsilon) + \nabla(\rho \varepsilon \mathbf{u}) = \nabla[\alpha_k \cdot \mu_{eff} \cdot \text{grad } \varepsilon] + C_{1\varepsilon}^* \cdot \frac{\varepsilon}{k} \cdot \tau_{ij} \cdot S_{ij} - C_{2\varepsilon} \cdot \rho \frac{\varepsilon^2}{k} \quad (3.6)$$

with;

$$\tau_{ij} = -\rho \overline{u'_i u'_j} = 2\mu_t S_{ij} - \frac{2}{3} \rho k S_{ij} \quad (3.7)$$

$$\mu_{eff} = \mu + \mu_t ; \mu_t = \rho C_\mu \frac{k^2}{\varepsilon} \quad (3.8)$$

$$C_\mu = 0.0845 , \alpha_k = \alpha_\varepsilon = 1.39 , C_{1\varepsilon} = 1.42 , C_{2\varepsilon} = 1.68 \quad (3.9)$$

where μ is dynamic viscosity, τ is stress components, k is turbulent kinetic energy, ε is dissipation rate [18].

3.2 Engine Model Setup

The engine selected for this study is Antor 6LD400 which is a single cylinder diesel engine with mechanical injection. The combustion chamber design of the engine is known as the Mexican hat design. The specifications of the engine are listed below.

Table 3.1 Specifications of the engine selected for this study

Engine Specification	Value
Manufacturer/Type	Antor 6LD400
Injection Type	Mechanical Injection
Number of Cylinders	1
Number of Strokes	4
Bore (mm)	86
Stroke (mm)	68
Displacement (cc)	395
Compression Ratio	18:1
Maximum Power (HP)	8.5
Maximum Torque (kgm)	2@2200 rpm
Combustion Chamber Type	Mexican Hat

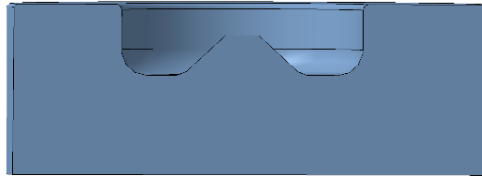


Figure 3.1 Mexican hat combustion chamber of Antor 6LD400

In this study, a new combustion chamber design concept has been introduced for Antor 6LD400. Within this concept, the piston bowl design of the engine has been changed into a so-called stepped lip chamber, which is a design that takes advantage of fuel targeting. The theory behind the stepped lip bowl and the numerical investigations for both the Mexican hat and the stepped lip bowls have been detailed in the following chapters.

3.2.1 Stepped Lip Combustion Chamber

The main purpose of stepped lip applications is to divide the fuel cone into two separate halves, directing a certain amount of it upwards to the cylinder head area and generating two separate combustion zones. Flame penetration to the squish volume is supported by directing the radial momentum of the upper portion of the fuel cone. Thus, decreased soot levels are achieved near the cylinder head where the soot emissions can be burned with the directed flame with the utilized air in the squish region. Additionally, more advanced fuel injection strategies can be achieved by multiple injection strategies, thus improving the air utilization inside the cylinder. Finally, due to the improved surface area-to-volume ratio, heat losses to the piston surface can be reduced [14].

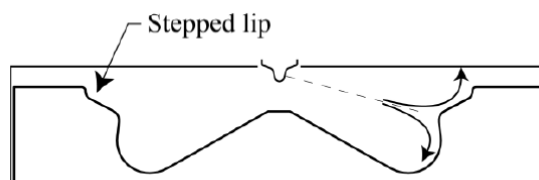


Figure 3.2 Illustration of the stepped lip combustion chamber

For further optimization of efficiency and emission levels of the stepped lip design, vortex formation mechanisms around the lip radius must be fully understood.

3.2.1.2 Vorticity Generation in Stepped Lip Combustion Chamber

The fuel separation and the vorticity generation starts with the fuel spray penetrating upwards and downwards toward the lip radius. Then, the fuel spray splits into two portions as it hits the bowl rim. The stepped surface directs the upper portion above the step and the spray gains a vertical velocity. The fuel separates from the piston surface as it reaches to the outer rim of the combustion chamber. The clockwise and counter-clockwise vortices appear between the piston and the cylinder head right after it separates from the combustion chamber [20].

A stepped lip bowl concept has been designed for Antor 6LD400 accordingly to the compression ratio of the engine. Bowl volume has been kept constant with the base Mexican model.

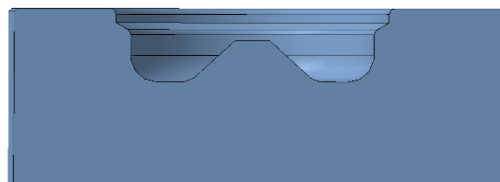


Figure 3.3 Stepped lip bowl design for Antor 6LD400

3.3 CFD Simulations

Ansys Forte has been used in this study for Cold Flow analyses of both combustion chamber models. The CFD model has simulated between the Inlet Valve Closure (IVC) and the Exhaust Valve Opening (EVO). Vortex formation mechanisms between two combustion chambers have been investigated and compared. The targeted locations are -50°CA , -25°CA and at TDC respectively. This is due to understanding the impact of piston geometry during the end of the compression

stroke since the effect of piston geometry during intake stroke and in the beginning of the compression is negligible.

Validation of the models has been made via a 1D simulation in GT Power with respect to the valve lifts in the Figure 3.4 given below. The valve lift timings are extracted from the workshop manual of the engine [21]. The timings are listed below.

Table 3.2 Valve timings of Antor 6LD400

Valve Action	Crank Degree
Intake valve opening	7,5° bTDC
Intake valve closing	25,5° aBDC
Exhaust valve opening	21° bBDC
Exhaust valve closing	3° aTDC

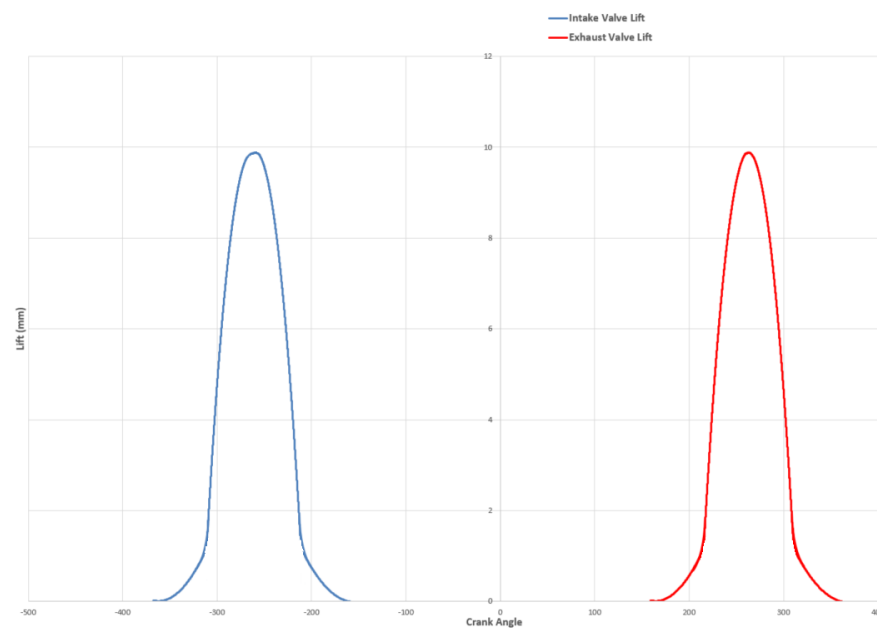


Figure 3.4 Valve lift profiles of Antor 6LD400

The in-cylinder pressure and temperature results obtained from the 1D analyses have given in the figures below.

The simulation started from the intake valve closing and ended at exhaust valve opening. The extracted data are taken from -50°CA bTDC, -25°CA bTDC and at

TDC respectively. This is due to understanding the impact of vortex formations once the fuel is injected into the combustion chamber since the injections are made with an advance.

Boundary conditions of the analysis is taken accordingly from the 1D analysis obtained from GT Power.

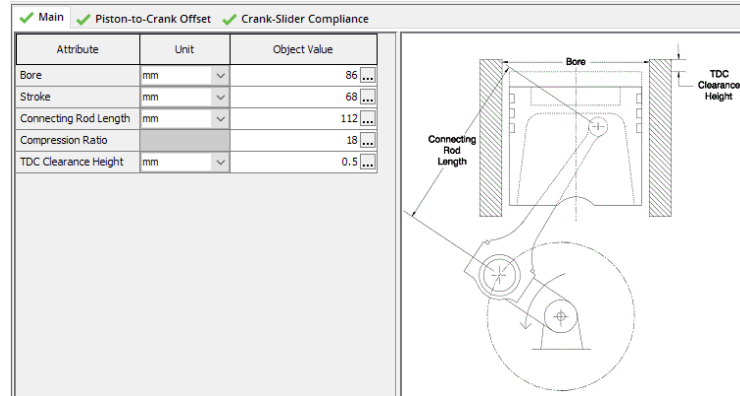


Figure 3.5 Illustration of GT Power interface

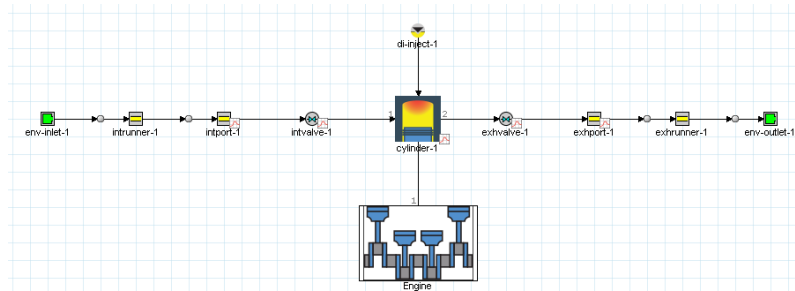


Figure 3.6 Illustration of the 1D model for the test engine

Table 3.3 Boundary conditions for CFD Analyses obtained from 1D analysis

Boundary Condition	Value
Initial Pressure (bar)	1
Engine Speed (rpm)	1500
Liner Temperature (K)	450 K
Piston Temperature (K)	590 K
Cylinder Head Temperature (K)	550 K

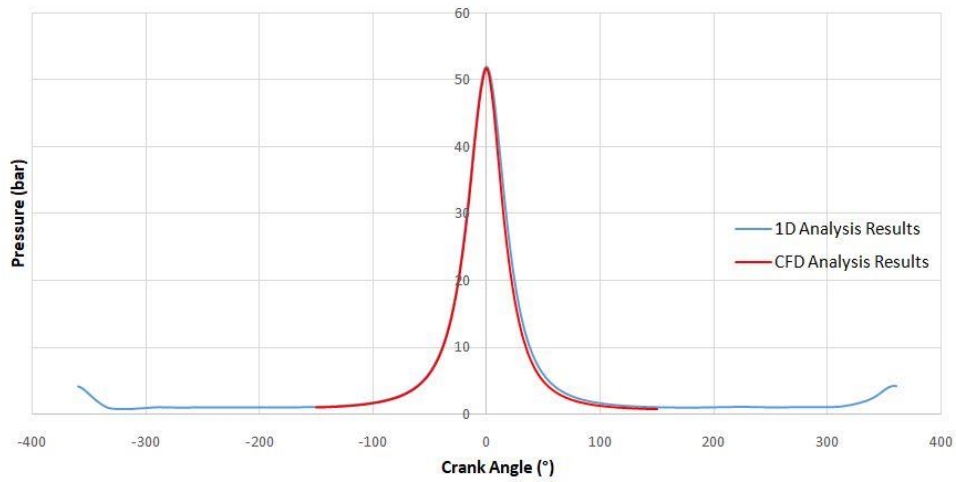


Figure 3.7 Validation of in-cylinder pressure between 1D and CFD analyses

3.4 CFD Results

The results obtained from -50° CA, -25° CA and at top dead center is detailed below.

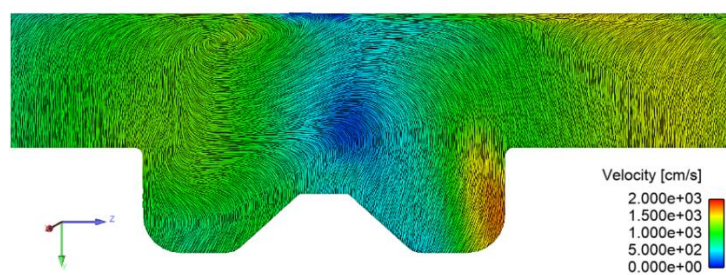


Figure 3.8 Mexican hat bowl at -50° CA

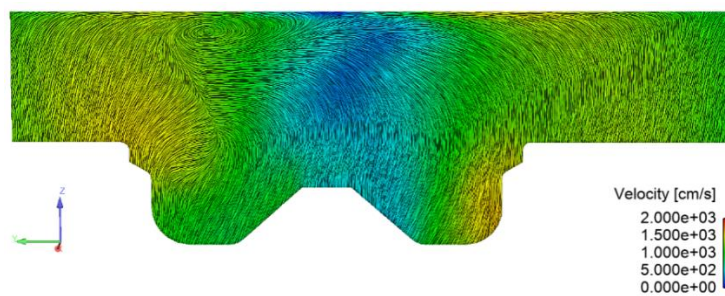


Figure 3.9 Stepped lip bowl at -50° CA

At -50° CA with the piston approaching top dead center, no significant difference is observed between two piston bowl geometries.

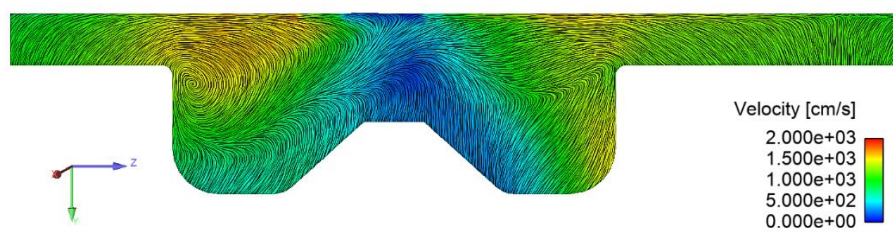


Figure 3.10 Mexican hat bowl at -25° CA

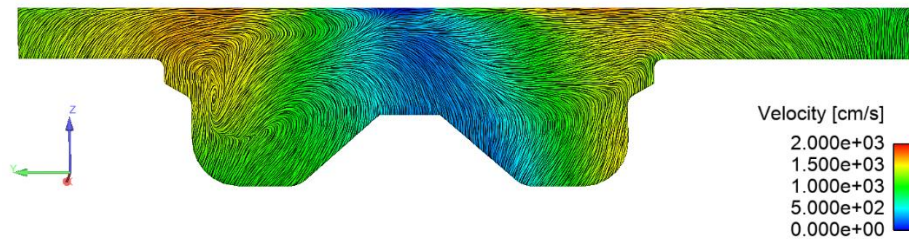


Figure 3.11 Stepped lip bowl at -25° CA

Both piston geometries are showing identical vortex formations at -25° CA. Although, the vortices formed in the stepped lip bowl are more disoriented compared to the more rounder vortices in mexican hat bowl.

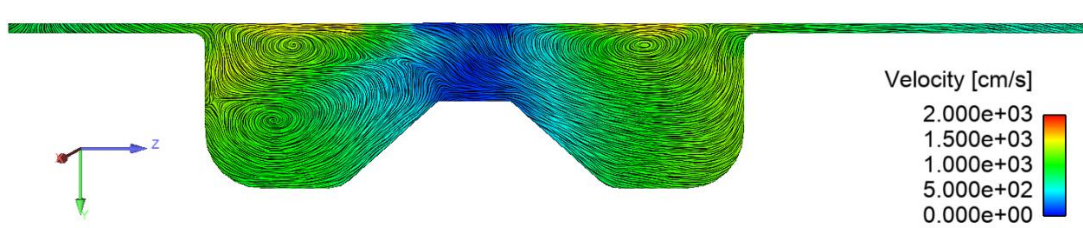


Figure 3.12 Mexican hat bowl at top dead center

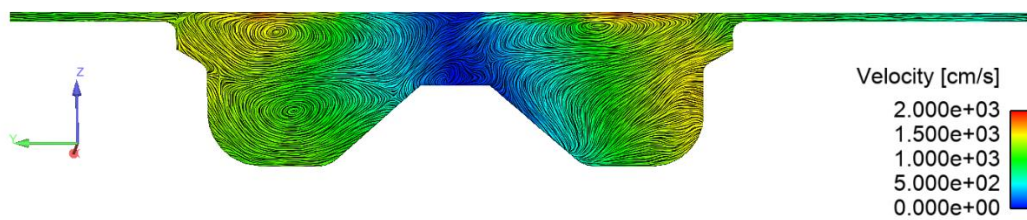


Figure 3.13 Stepped lip bowl at top dead center

Distinguishable differences in both piston designs can be seen while the pistons are at top dead center. The vortices in the mexican hat bowl are shown in more rounder patterns while the vortices in the stepped lip bowl are more wider and tilted over the squish area.

Although the cold flow analyses gave an information about the in cylinder vortex formation mechanism, more detailed investigations of the chambers have to be made experimentally with fuel injection. This is due to understanding the effect of fuel separation that occurs via the lip radius in the stepped lip combustion chamber design. The experimental part of this particular study is detailed in the next chapter.

EXPERIMENTAL WORK

The specifications of the selected engine for this study were shared in the previous chapter. In this chapter, the details of the emission measurement system and the dynamometer being used for testing is explained briefly. The methodology behind the piston production process is mentioned in this chapter as well.

4.1 Methodology Used for Piston Production

2 base model pistons have been purchased from the aftermarket and one piston has been machined accordingly to a stepped lip piston design. The machining dimensions and tolerances are given in the Figure 4.1 below.

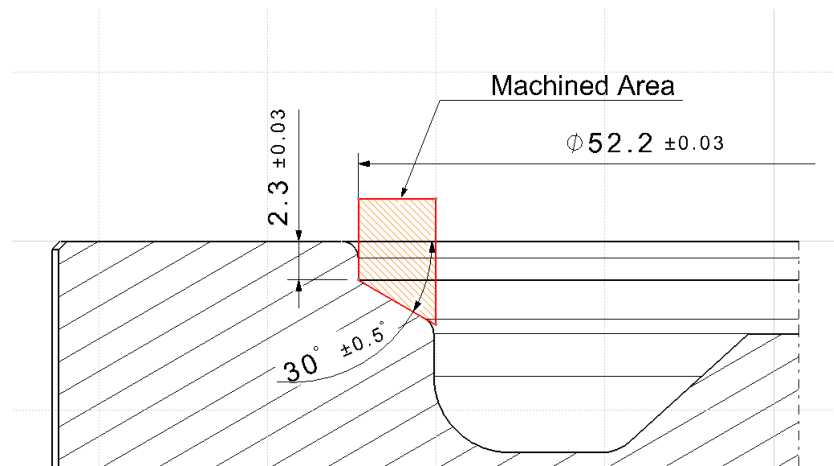


Figure 4.1 Machining dimensions and tolerances for stepped lip design

For precise compression ratio calculations, since the dead volume of the engine when the piston is at top dead center is unknown, this value (V_{dead}) is calculated first.

$$r_c = 18 = \frac{V_{bowl} \pm V_{dead} \pm V_{engine}}{V_{bowl} \pm V_{dead}} \quad (4.1)$$

with;

$$V_{engine} = \frac{\pi}{4} (Bore^2) Stroke \quad (4.2)$$

$$V_{engine} = \frac{\pi}{4} \cdot 86^2 \cdot 68 = 394799 \text{ mm}^3 \quad (4.3)$$

and;

$$V_{bowl} = 16500 \text{ mm}^3 \quad (4.4)$$

V_{dead} is calculated as;

$$18 = \frac{16500 + V_{dead} + 394799}{16500 + V_{dead}} \quad (4.5)$$

$$V_{dead} = 6723 \text{ mm}^3 \quad (4.6)$$

With machining the piston into the stepped lip desing, the bowl volume increased to 18,9 cc. The compression ratio of the engine for the new model is calculated below.

$$r_{c_{new}} = \frac{18900 + 6723 + 394799}{18900 + 6723} = 16.4 \quad (4.7)$$



Figure 4.2 Machining process of stepped lip bowl



Figure 4.3 Machined stepped lip combustion chamber

For testing purposes, the second piston is machined from its top surface while keeping to bowl diameter constant. In order to calculate the required machining dimension, a parametrical model for the newpiston bowl volume ($V_{new\ bowl}$) of the base piston is introduced since both the clearance volume and the bowl volume is changing in this process. The technical drawing of the parametrical model of the base piston for 0,55 mm machining is shown below. As for the compression ratio calculation, the clearance volume $V_{clearance}$ is added into the equation.

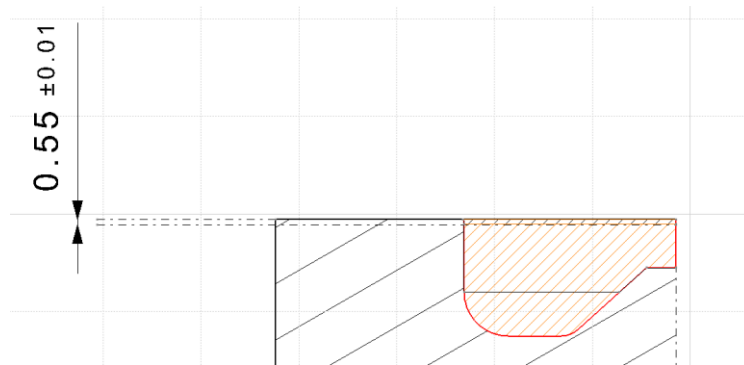


Figure 4.4 Technical drawing of the parametric bowl volume for 0.55 mm machining

$$r_c = \frac{V_{new\ bowl} + V_{dead} + V_{engine} + V_{clearance}}{V_{new\ bowl} + V_{dead} + V_{clearance}} \quad (4.8)$$

$$V_{clearance} = \frac{\pi}{4} \cdot (86^2) \cdot 0,55 = 3193\text{mm}^3 \quad (4.9)$$

The bowl volume for the second design is calculated as 15670 mm³ from the parametrical model. Finally, for validation purposes, the compression ratio for 0,55 mm machining is given below.

$$r_c = \frac{15670+6723+394799+3193}{15670+6723+3195} = 16,4 \quad (4.10)$$



Figure 4.5 Top surface machining process of the second piston

4.2 DC Motor Specifications

The DC driver selected for this study is FEMSAN K.10.S28. The engine is loaded in targeted operating speeds and; the voltage and current levels are obtained to calculate power and torque characteristics of the engine. The specifications of the DC driver is listed in the table below.



Figure 4.6 Selected DC motor for experimental work

Table 4.1 Specification of DC Motor

Specification	Value
Type	FEMSAN K.10.S28
Power (kW)	15
Torque (Nm)	68
Maximum revolution (rpm)	4000
Cooling type	IC06 Fan mounted on the motor
Working regime	S1
Armature voltage (V)	440
Exciter output (W)	600
Efficiency	90%

4.3 Specifications of Emission Measurement Devices

AVL DiGas 4000 has been selected for CO, CO₂, HC, NO_x and O₂ emission measurement. AVL Digas 4000 is capable of measuring CO, CO₂ and NO_x emissions by infrared methods and, NO_x and O₂ by electrochemical methods. Specifications of AVL Digas is listed in the table below.

Table 4.2 Specifications of AVL Digas 4000

Measurement	Measuring Range	Sensitivity
Engine Speed	250-8000 rpm	10 rpm
Oil temperature	0-120°C	1°C
CO	0-10% (volumetric)	0,01%
CO ₂	0-20% (volumetric)	0,1%
HC	0-20000 ppm (volumetric)	1 ppm
O ₂	0-22% (volumetric)	0,1%
NO _x	0-4000 ppm (volumetric)	1 ppm

AVL Digas 4000 emission measurement device uses nondispersive infrared analyzer (NDIR) for CO and CO₂ emissions, flame ionization detector (FID) for HC emissions, paramagnetic analyzer for O₂ emissions and chemiluminescence detector (CLD) for NO_x emissions.

NDIR method utilizes the total infrared radiation absorption of CO and CO₂ molecules. FID measures the current output generated by HC emissions that goes through a nonionized hydrogen flame. Paramagnetic analyzers which are used for O₂ emission measurement measures the magnetic force generated by the diversion of O₂ molecules under a magnetic field. CLD measures the light generated via the NO₂ formation from the NO_x gases.

AVL 415S is selected in order to measure the soot levels for both combustion chambers. AVL 415S filters the exhaust gas samples collected from the exhaust line and measures the opacity of the filter paper and gives out an output in Filter Smoke Number (FSN). The specifications of the device is listed in the table below.

Table 4.3 Specifications of AVL 415S

Specification	Unit
Measuring method	Opacity level of filter paper
Output unit	FSN – mg/mm ³
Measuring range	0-10 FSN
Operating temperature	5-55°C
Sensitivity	0.002 FSN-0.02 mg/m ³
Resolution	0.001 FSN-0.01 mg/m ³
Repeatability	≥ 0.05 FSN
Operating humidity range	≤ 95% without condensation
Exhaust gas pressure	-100-+400 mbar
Exhaust gas temperature	600°C

The measured FSN values can be converted into mg/m³ by using a correlation equation. The correlation equation is given below. [27]

$$C \left(\frac{\text{mg}}{\text{m}^3} \right) = \frac{1}{0.405} \cdot 4,95 \cdot \text{FSN} \cdot \exp(0,38 \cdot \text{FSN}) \quad (4.3)$$

4.4 Engine Operation Conditions

After assembling the pistons, all engines ran 2 hours at the idle position. This was due to obtaining more reliable emission results since the piston rings were brand new in all assemblies.

For the experiments, due to the limitations caused by the speed governor of the engine, we observed major speed fluctuations under 2600 rpm with ± 100 rpm. Additionally, above the 3600 rpm range the engine was not able to produce enough power in order to make a reliable comparison. Considering our limitations, the engine has been loaded from its maximum speed and held constant at 2 separate power and speed conditions selected between our

limitation range. The selected operation points are listed at the table below. All emissions are obtained after waiting 5 minutes at the specified conditions.

Table 4.4 Steady state experiment conditions

Experiment No	Engine Speed (rpm)	Power Output (kW)	BMEP (bar)
1	3000	2,4	2,4
2	2800	3,3	3,5

4.5 Emission Results

Each emission results obtained from all three combustion chambers are shown in the figures below. In the figures, MH stands for mexican hat combustion chamber and SL stands for stepped lip combustion chamber. Additionally the compression ratios of each bowl are given as CR 18 and CR 16,4 in the figures.

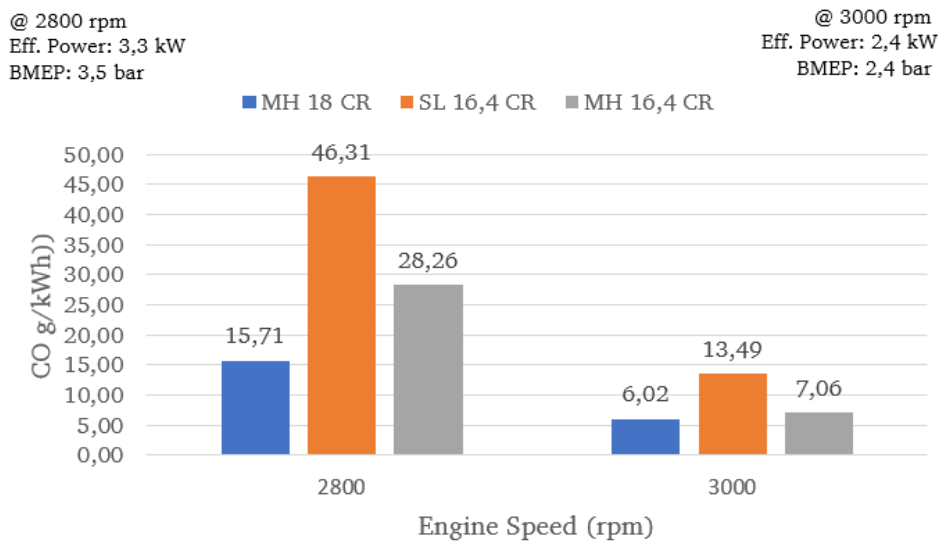


Figure 4.7 CO Emission results

It can be seen from the Figure 4.5.1 that the stepped lip bowl increased the CO emissions 65% and 100% in 2800 rpm and 3000 rpm respectively compared with the mexican hat bowl with the same compression ratios. An increase in emissions compared to the mexican hat bowl with 18:1 compression ratio is expected due to lower compression temperatures.

@ 2800 rpm
Eff. Power: 3,3 kW
BMEP: 3,5 bar

@ 3000 rpm
Eff. Power: 2,4 kW
BMEP: 2,4 bar

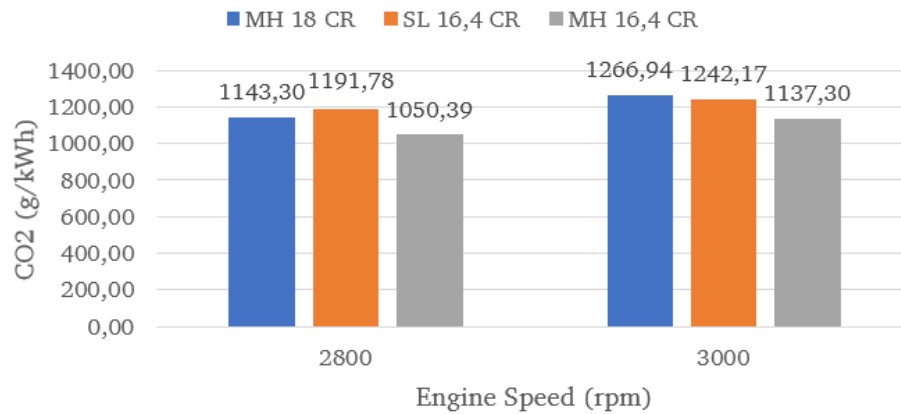


Figure 4.8 CO₂ Emission results

Although the CO₂ emissions remained identical for each combustion chamber at 3000 rpm, 13% increase in 2800 rpm for the stepped lip bowl has been observed.

@ 2800 rpm
Eff. Power: 3,3 kW
BMEP: 2,4 bar

@ 3000 rpm
Eff. Power: 2,4 kW
BMEP: 2,4 bar

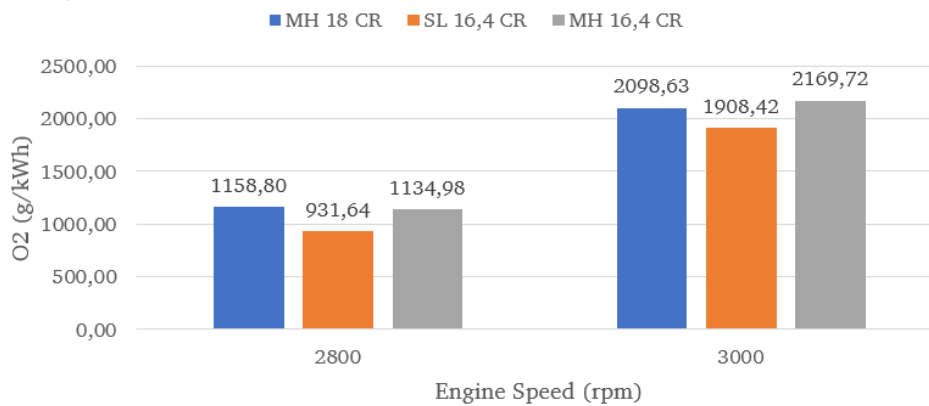


Figure 4.9 O₂ Emission results

The O₂ emissions remained almost constant at 3000 rpm for all three combustion chambers but a slight decrease with 17% has been measured with the stepped lip bowl at 2800 rpm.

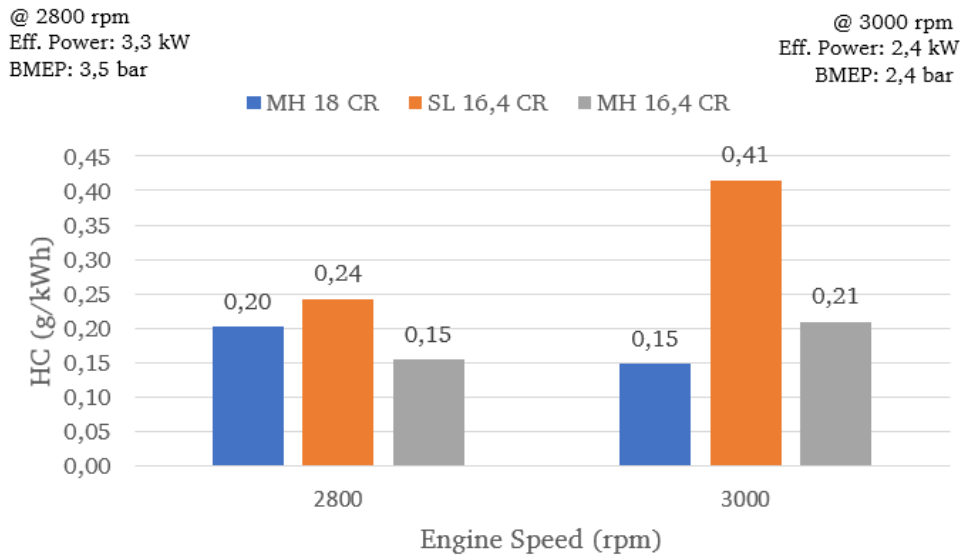


Figure 4.10 HC Emission results

For the results obtained for HC emissions, it can be seen that the stepped lip bowl geometry has strongly increased the emissions with 60% at 2800 rpm and 100% at 3000 rpm compared with the mexican hat bowl with the same compression ratio.

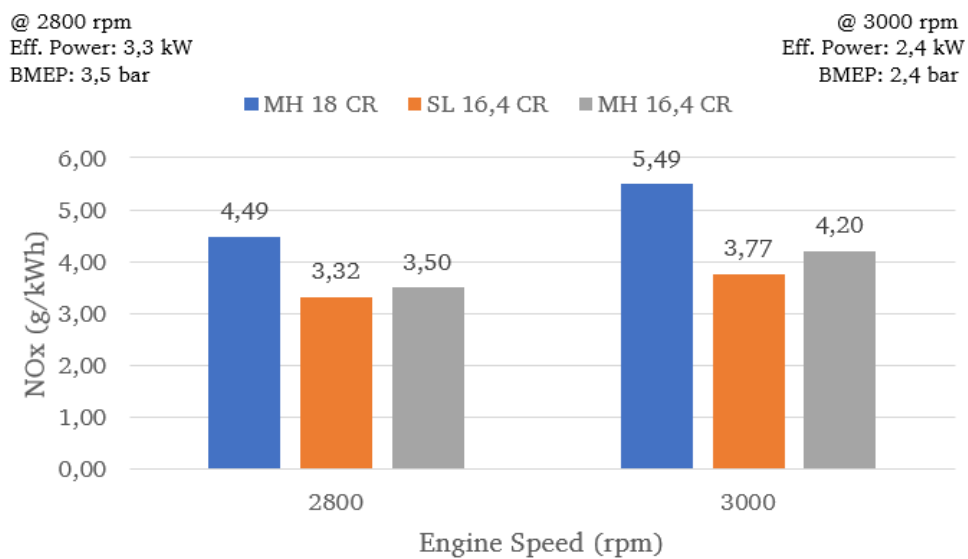


Figure 4.11 NO_x Emission results

Although it is expected to see a decrease in NO_x emissions in the Figure 4.5.5 due to lowered compression ratio; it seems that there is no significant difference in NO_x emissions between the stepped lip bowl and the mexican hat bowl under all operation conditions.

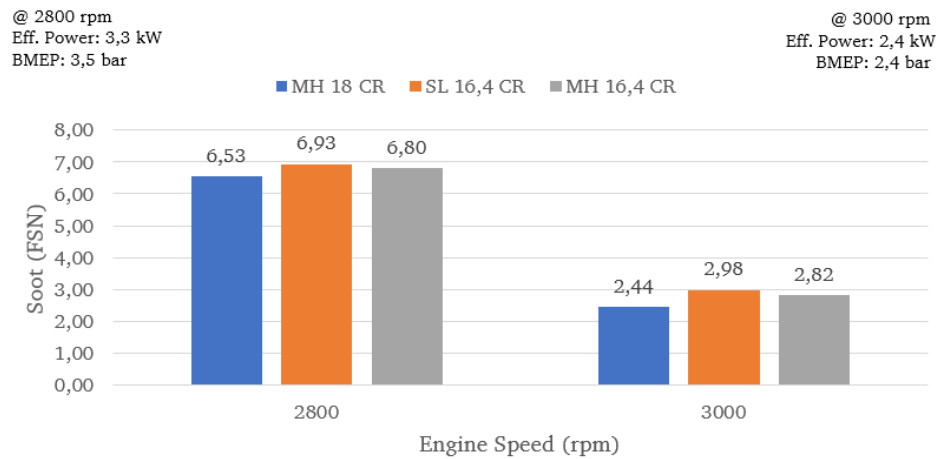


Figure 4.12 Soot emission results

Since the compression temperatures are lowered from 18:1 to 16,4:1; it is expected to see an increase in soot emissions with 6% at 2800 rpm and 22% at 3000 rpm. There were no significant difference between the stepped lip and mexican hat combustion chambers with the same compression ratio.

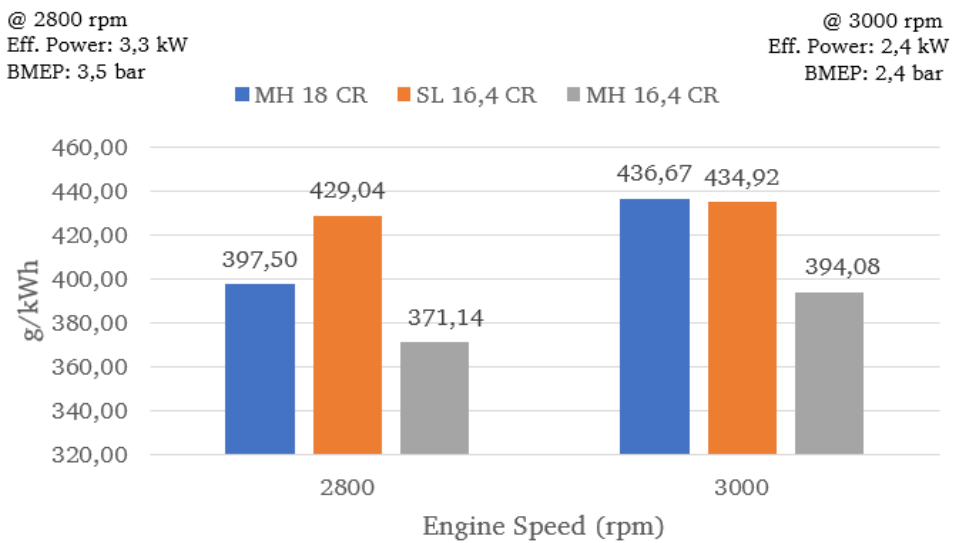


Figure 4.13 Calculated fuel consumption results

In 2800 rpm, 8% increase observed with lowered compression ratio in the stepped lip bowl. Comparisons between the stepped lip bowl and the mexican hat bowl 16% increase at 2800 rpm and 10% increase in 3000 rpm is observed.

RESULTS AND DISCUSSION

- i. In cold flow analyses, there were no significant difference at -50° CA BTDC and -25° CA BTDC positions with either combustion chamber. Differences in stepped lip design are observed with the pistons are at TDC. The vortices in the stepped bowl were more wider and tilted over the squish area which can indicate the stepped lip combustion chamber can utilize the air in the squish region once the fuel is injected.
- ii. Increased CO and HC emissions indicated that the lower injection pressures and in-cylinder temperatures in mechanical injection engines strongly affected the emission formations more than the combustion chamber geometry with the addition of lowered compression ratios. The reason behind increased CO and HC levels in stepped bowl compared to mexican hat in the same compression ratio situation may be the flame quenching of the upper portion which is directed via the lip radius.
- iii. There no significant difference in soot emission levels between the stepped lip and the mexican hat combustion chambers. It can be said that the low injection pressures and low in-cylinder pressures and temperatures have a more dominant factor on the combustion process of a mechanical injection engine rather than the geometrical shape of the combustion chamber.
- iv. To be able to better understand and make a comment about the emission characteristics of the engine, in-cylinder pressure must be measured and analyzed. On this matter, the material selection for the cylinder head has narrowed our limitations. Even in the experimental part of the study, the threads at the exhaust side of the cylinder head were severely damaged.
- v. In order to have a better understanding of emission formation in the test engine, a combustion CFD model must be build including the injector parameters such as cone angle, injector protrusion and injection advance so that the fuel targeting aspect of stepped lip bowl is fully understood.

- vi. The future studies for the selected test engine can include optimizing the valve lift profiles and injection parameters to decrease emission levels.
- vii. The future studies can include, experimenting the stepped lip combustion chamber with an engine which has wider bowl diameters and air charging system.

REFERENCES

- [1] F. Leach, R. Ismail, M. Davy, A. Weall ve B. Cooper, «The effect of a stepped lip piston design pn performance and emissions from a high speed diesel engine,» *Applied Energy*, pp. 679-689, 2015.
- [2] J. Styron, B. Baldwin, B. Fulton, D. Ives ve S. Ramanathan, «Ford 2011 6.7L Power Stroke Diesel Engine Combustion System Development,» *SAE Technical Papers*, 2011.
- [3] J. Benajes, V. Pastor, A. Garcia ve J. Monsalve-Serrano, «An experimental investigation on the influence of piston bowl geometry on RCCI perfromance and emissions in a heavy-duty engine,» *Energy Conservation and Management*, pp. 1019-1030, 2015.
- [4] F. Perini, K. Zha, S. Busch, E. Kurtz, R. C. Peterson, A. Warey ve R. D. Reitz, «Piston geometry effects in a light duty, swirl supported diesel engine: Flow structure characterization,» *International Journal of Engine Research*, pp. 1079-1098, 2018.
- [5] T. Eder, M. Kemmer, P. Lückert ve H. Sass, «OM-654 - Launch of a New Engine Family by Mercedes-Benz».
- [6] J. Lee, S. Lee, J. Kim ve D. Kim , «Bowl shape design optimization for engine-out PM reduction in heavy duty diesel engine,» *SAE Technical Papers*, 2015.
- [7] J. G. Dolak, Y. Shi ve R. D. Reitz, «A computational investigation of stepped-bowl piston geometry for a light duty engine operations at low load,» *SAE Technical Papers*, 2010.
- [8] J. Dahlstrom, O. Andersson ve M. Tuner, «Experimental comparison of heat losses in stepped-bowl and re-entrant combustion chambers in a light duty diesel engine,» *SAE Technical Papers*, 2016.
- [9] J. B. Heywood, *Internal Combustion Engine Fundamentals*, 2nd Edition, McGraw-Hill , 2018.
- [10] W. W. Pulkrabek, *Engineering Fundamentals of the Internal Combustion Engine*, 2nd Edition, Pearson, 2003.

- [11] O. Özener, Dizel Motorlarında Pilot Püskürtmenin Performans ve Emisyon Açısından Optimizasyonu, Doctorate Thesis, Yıldız Technical University, 2013.
- [12] P. A. Lakshminarayanan ve Y. V. Aghav, Modelling Diesel Combustion, Springer, 2010.
- [13] C. Baumgarten, Mixture Formation in Internal Combustion Engines, Springer, 2006.
- [14] C. Miles ve Ö. Andersson, «A review of design considerations for light-duty diesel combustion systems,» *International Journal of Engine Research*, pp. 6-15, 2016.
- [15] P. A. Lakshminarayanan ve A. K. Agarwal, Design and Development of Heavy Duty Diesel Engines, Springer, 2020.
- [16] T. Zhang, J. Eismark, K. Munch ve I. Denbratt, «Effects of a wave-shaped piston bowl geometry on the performance of heavy duty diesel engines fueled with alcohols and biodiesel blends,» *Renewable Energy*, pp. 512-522, 2019.
- [17] X. Li, H. Zhou, L. Su ve Y. Chen , «Combustion and emission characteristics of a lateral swirl combustion system for DI diesel engines under low excess air ratio conditions,» *Fuel*, pp. 672-680, 2016.
- [18] N. A. Shafie ve M. F. Said, «Cold flow analysis on internal combustion engine with different piston bowl configurations,» *Journal of Engineering Science and Technology*, pp. 1048-1066, 2017.
- [19] H. K. Versteeg ve W. Malalasekera, An Introduction to Computational Fluid Dynamics, Second Edition, Pearson, 2007.
- [20] S. Busch ve F. Perini, «Progress toward understanding vortex generation in stepped-lip diesel engine combustion chambers,» *Results in Engineering*, Article 100004, 2009.
- [21] Workshop Manual, Lombardini Inc., 1990.
- [22] F. Tian ve J. Abraham, «Application of computational fluid dynamics (CFD) in teaching internal combustion engines,» *International Journal of Mechanical Engineering*, pp. 73-83, 2014.
- [23] Q. Luo, X. Si ve H. Yin, «Application of CFD technology in the development and research of internal combustion engines,» *International Conference on Computer and Information Technology Applications*, 2016.

- [24] G. Martinas , O. S. Cupsa, L. C. Stan ve A. Arsenie, «Cold flow simulation of an internal combustion engine with vertical valves using layering approach,» *IOP Conference Series: Materials Science and Engineering*, 2015.
- [25] D. Güneş ve M. S. Horasan, «Full cycle cold flow analysis of the effect of twin swirl combustion chamber design in a diesel engine,» *World Journal of Mechanics* , pp. 109-117, 2016.
- [26] J. V. Pastor, A. Garcia, C. Mico ve F. Lewiski, «Soot reduction for cleaner compression ignition engines through innovative bowl templates,» *International Journal of Engine Research*, pp. 1-15, 2020.
- [27] W. F. Northrop, S. V. Bohac, J. Y. Chin ve D. N. Assanis, «Comparison of filter smoke number and elemental carbon mass from partially premixed low temperature combustion in a direct-injection diesel engine,» *Journal of Engineering for Gas Turbines and Power*, Article: 102804, 2011.

PUBLICATIONS FROM THE THESIS

Conference Papers:

1. C. Karaca, L. Yüksek, “Design and Analysis of a Low Soot Emission Targeted Combustion Chamber in Diesel Engines”, 7th International Congress on Engineering, Architecture and Design, 2021, pp 690-697